

Review

Detection of Oxidative Stress Induced by Nanomaterials in Cells—The Roles of Reactive Oxygen Species and Glutathione

Jan Čapek *  and Tomáš Roušar 

Department of Biological and Biochemical Sciences, Faculty of Chemical Technology, University of Pardubice, Studentska 573, 532 10 Pardubice, Czech Republic; Tomas.Rousar@upce.cz

* Correspondence: jan.capek7@upce.cz; Tel.: +420-466-037-717

Abstract: The potential of nanomaterials use is huge, especially in fields such as medicine or industry. Due to widespread use of nanomaterials, their cytotoxicity and involvement in cellular pathways ought to be evaluated in detail. Nanomaterials can induce the production of a number of substances in cells, including reactive oxygen species (ROS), participating in physiological and pathological cellular processes. These highly reactive substances include: superoxide, singlet oxygen, hydroxyl radical, and hydrogen peroxide. For overall assessment, there are a number of fluorescent probes in particular that are very specific and selective for given ROS. In addition, due to the involvement of ROS in a number of cellular signaling pathways, understanding the principle of ROS production induced by nanomaterials is very important. For defense, the cells have a number of reparative and especially antioxidant mechanisms. One of the most potent antioxidants is a tripeptide glutathione. Thus, the glutathione depletion can be a characteristic manifestation of harmful effects caused by the prooxidative-acting of nanomaterials in cells. For these reasons, here we would like to provide a review on the current knowledge of ROS-mediated cellular nanotoxicity manifesting as glutathione depletion, including an overview of approaches for the detection of ROS levels in cells.

Keywords: reactive oxygen species; oxidative stress; glutathione; nanotoxicity; cell injury; fluorescence probes



Citation: Čapek, J.; Roušar, T. Detection of Oxidative Stress Induced by Nanomaterials in Cells—The Roles of Reactive Oxygen Species and Glutathione. *Molecules* **2021**, *26*, 4710. <https://doi.org/10.3390/molecules26164710>

Academic Editor: Pál Perjési

Received: 1 July 2021

Accepted: 2 August 2021

Published: 4 August 2021

Publisher's Note: MDPI stays neutral with regard to jurisdictional claims in published maps and institutional affiliations.



Copyright: © 2021 by the authors. Licensee MDPI, Basel, Switzerland. This article is an open access article distributed under the terms and conditions of the Creative Commons Attribution (CC BY) license (<https://creativecommons.org/licenses/by/4.0/>).

1. Introduction

Molecular oxygen (O_2) has a significant effect on numerous chemical reactions and biological processes. O_2 reductions are one of the most critical electrocatalytic reactions that function in electrochemical energy conversion [1]. Free radicals contain an unpaired electron mostly bound to oxygen atoms. Conversely, the group of compounds named reactive oxygen species (ROS) also contains molecules without an unpaired electron, e.g., hydrogen peroxide [2,3]. Thus, the group of ROS also contains oxygen free radicals such as superoxide or hydroxyl, alkoxyl, peroxy, and nitroxyl radicals [4,5]. The production of ROS is commonly linked with mitochondria, where the electrons are transferred through the respiratory chain to O_2 forming water [6,7]. Mitochondrial ROS production depends on many factors such as the membrane potential of mitochondria [8], concentration of mitochondrial respiratory substrates, or a type of cells [9]. Mitochondria are the most important sources of superoxide and hydrogen peroxide in mammalian cells. The production of these ROS occurs mainly on the mitochondrial respiratory complex I and III [7,10]. In addition to mitochondrial complexes, ROS is also produced in mammalian cells by the participation of other enzymes such as flavoproteins [11] and other enzymes involved in nutrient metabolism [12]. As ROS plays important roles in the regulation of cell death processes, i.e., apoptosis [13] or necrosis [14–16], their pathological roles have been identified in a number of diseases including cancer and other age-related degenerative processes [17,18]. Given their deleterious effects, ROS production is usually finely tuned by ROS-scavenging systems [9].

Nanomaterials (NMs) exhibit great potential for use in the biomedical, optical, and electronic fields [19–23]. However, nanomaterials have been considered as potentially toxic due to their unique properties. They have extremely high surface-to-volume ratios, making them very reactive and catalytically active [24]. Their toxic potential in cells is also supported by their small size, enabling them to easily penetrate cell membranes [25]. TiO₂ is one of the most commonly used nanomaterials in the chemical industry (e.g., cosmetics and pigments) [26]. In addition to white lead properties, TiO₂ can be very active in photocatalytic reactions with organic compounds, providing the formation of ROS including •OH, O₂•[−], H₂O₂ [27]. In addition to TiO₂, other nanomaterials of different chemical compositions can produce ROS. The overview of NMs capable of ROS production is summarized in Table 1 including the lifetime.

Table 1. Overview of nanomaterials capable of ROS production [28].

Nanomaterial	Produced ROS	ROS	Half-Life
ZnO [29], SiO ₂ [29], TiO ₂ [30], CuO [31], Ag NPs [32]	Superoxide	O ₂ • [−]	10 ^{−6} s
ZnO [33], TiO ₂ [34], CuO [35]	Hydroxyl radical	•OH	10 ^{−10} s
Polystyrene NPs [36], Au NPs [37], TiO ₂ [38], ZnO [39], Ag NPs [40]	Hydrogen peroxide	H ₂ O ₂	Stable (x.s, min)
TiO ₂ [41], Ag NPs [42], FeO [43]	Singlet oxygen	¹ O ₂	10 ^{−6} s

Nanomaterials or nanoparticles (NPs) can expose transition metals on their surface, which can generate ROS through Fenton or Haber-Weiss reactions [44]. During these reactions, hydrogen peroxide is reduced in the presence of transition metals (Fe²⁺, Cu⁺) to form a highly active and toxic hydroxyl radical. Thus, the role of nanomaterials in ROS-mediated cell damage is significant and ROS production induced by NMs can lead to the modulation of various intracellular pathways, e.g., NF-κB, caspases, MAPK, etc., involving the activation of cell death processes [45,46].

In this study, we aimed to provide a recent and detailed view on ROS production induced by nanomaterials. The importance of our review can be also supported by the role of increased ROS levels that can lead to glutathione depletion and to the activation of cellular signaling pathways, resulting in changes in cellular metabolism, cell damage, or even in cell death.

2. Reactive Oxygen Species

2.1. Superoxide

Superoxide radical is formed during enzymatic and non-enzymatic reactions in biological systems [1,47]. In atoms and molecules, paired electrons occur usually as antiparallel, which strongly limits the oxidation properties of O₂. After one-electron reduction of molecular oxygen, the superoxide radical (O₂•[−]) forms. This reaction is thermodynamically very unfavorable and the interaction of O₂ with another paramagnetic center is important for overcoming spin restriction [48]. Although the reactivity of O₂•[−] is mild, the crucial role of superoxide is that it enables the formation of other ROS (Figure 1), playing important roles in the pathology of various diseases.

Superoxide radical (O₂•[−]) is formed mainly in mitochondria and its reactivity with biomolecules is relatively low. Superoxide can be produced after the reaction of molecular oxygen with divalent metals catalyzing a single-electron reduction under their simultaneous oxidation (equation 1).



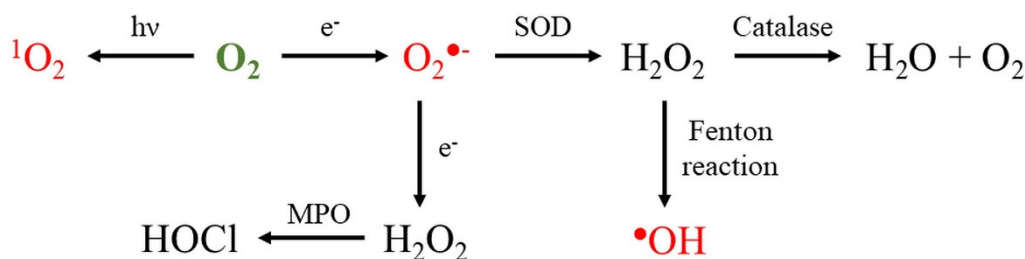


Figure 1. Formation of reactive oxygen species. Abbreviations: SOD = superoxide dismutase; MPO = myeloperoxidase; O_2 = oxygen; 1O_2 = singlet oxygen; $O_2^{\bullet-}$ = superoxide; H_2O_2 = hydrogen peroxide; $\bullet OH$ = hydroxyl radical; HOCl = hypochlorous acid; and $h\nu$ = radiation. ROS colored in red are free oxygen radicals.

Another formation can be catalyzed by enzymes including xanthine oxidase, lipoxigenase, or cyclooxygenase [49]. The superoxide radical may exist in two possible forms: either in the form of $O_2^{\bullet-}$ at physiological pH or as a hydroperoxyl radical (HO_2^{\bullet}) at low pH levels [50]. Hydroperoxyl radical penetrates better through phospholipid bilayers compared to the charged form $O_2^{\bullet-}$ [28,51]. The superoxide radical may react with another superoxide radical to form hydrogen peroxide and O_2 (equation 2). The reaction is catalyzed by the enzyme superoxide dismutase (SOD) [52,53]. A product of the dismutation reaction is H_2O_2 which becomes an important factor in the formation of the most reactive ROS, i.e., hydroxyl radical ($\bullet OH$) [54].



The mitochondrial electron transport chain (ETC) has been attributed to the role as the main ROS generator in cells. When transporting electrons, some of the electrons from the ETC can reduce molecular oxygen to $O_2^{\bullet-}$ [55]. The resulting $O_2^{\bullet-}$ is rapidly dismissed by mitochondrial superoxide dismutase (Mn-SOD) forming H_2O_2 [56]. Mitochondrial ETC consists of several electron transporters (flavoproteins, proteins containing iron and sulfur, ubiquinone, and cytochromes) with redox potentials ranging from -0.200 to $+0.600$ V [57,58]. According to the respective redox potentials, the individual electron carriers are arranged in individual complexes of the respiratory chain I–IV. Electrons that are transported into the respiratory chain as reducing equivalents of NADH or $FADH_2$ enter the ETC through mitochondrial Complexes I and II. Then, the electrons are transferred through ETC to Complex IV which reduces O_2 to H_2O . From the thermodynamical perspective, all these electron transport systems could transfer the electrons directly to O_2 to form $O_2^{\bullet-}$. However, there are only two major sites of the respiratory chain where ROS can be generated, i.e., at Complexes I and III [59,60].

In Complex I, a reaction occurs between O_2 and the reduced form of the flavinmononucleotide (FMN), leading to production of $O_2^{\bullet-}$. The amount of reduced FMN depends on the NADH/NAD⁺ ratio [61]. In Complex III, two specific binding sites for coenzyme Q10 are known, i.e., Q_i and Q_o . Superoxide production is located in Q_o . When antimycin A is added as an inhibitor of the Q_i site, $O_2^{\bullet-}$ production increases [62], while the addition of a myxothiazole inhibitor for the Q_o site decreases ROS production [63]. Under physiological conditions, the production of ROS in Complex III depends on the $\Delta\Psi$. The rate of $O_2^{\bullet-}$ formation may increase exponentially with increasing $\Delta\Psi$. This directly correlates with the fact that due to $\Delta\Psi$ fluctuations, the transport of electrons from heme bL to heme bH slows down, which then increases superoxide generation [64].

2.1.1. Role of Superoxide in Nanomaterial Toxicity

Damage to mitochondria and subsequent ROS leakage is a commonly accepted mechanism of nanoparticles toxicity. Damaged mitochondria release $O_2^{\bullet-}$ into the intermembrane space which can ultimately damage the cell [65]. Across different types of nanomaterials, their involvement in the ROS generation can be found. Far more often

than in size, their possible cytotoxic effects are chemically dependent. Despite the similar size and crystal shape of ZnO NPs and SiO₂ NPs, higher toxicity of ZnO NPs is observed, where cell viability is reduced and O₂^{•−} generation is reduced, due to which glutathione (GSH) depletion occurs [29]. TiO₂ nanoparticles generate O₂^{•−} [30] both in solution and in cells, and intracellular O₂^{•−} reduces the expression of histone deacetylase 9 (HDAC9), an epigenetic modifier [66]. Cellular internalization of TiO₂ NPs has been shown to activate macrophages and neutrophils contributing to the production of O₂^{•−} by the NADPH oxidase [67]. Oxidative stress induced by excessive O₂^{•−} production is an important mechanism of the CuO NPs toxicity [31]. CuO NPs can enter HepG2 cells, where they are capable of inducing cellular toxicity by generating O₂^{•−} leading to GSH depletion [68]. Activation of mitogen-activated protein kinases (MAPKs) and redox-sensitive transcription factors was demonstrated, suggesting that MAPK pathways and redox-sensitive transcription factors could be major factors of CuO NPs toxicity [69].

Analysis of mouse fibroblasts and human hepatocytes revealed that an increase in ROS levels induced by Ag NPs is accompanied by a reduction of mitochondrial membrane potential, release of cytochrome c into the cytosol, JNK activation, and translocation of Bax to mitochondria [32]. After exposure to Ag nanoparticles, GSH depletion occurs in liver cells, which is directly related to ROS production [70]. Ag NPs appear to induce DNA damage through a mechanism involving ROS production.

2.1.2. Methods for the Detection of Superoxide

MitoSox

Hydroethidium (HE) is a selective O₂^{•−} detection probe (Figure 2) that reacts very rapidly to changes in O₂^{•−} concentration, forming a red fluorescent product with 2-hydroxyethidium cation (2-OH-E⁺). Hydroethidine is a reduced form of ethidium that can be oxidized to ethidium in cells. The resulting ethidium intercalates nucleic acids and significantly increases its fluorescence, emitted at 610 nm (excitation = 535 nm) [23,71].

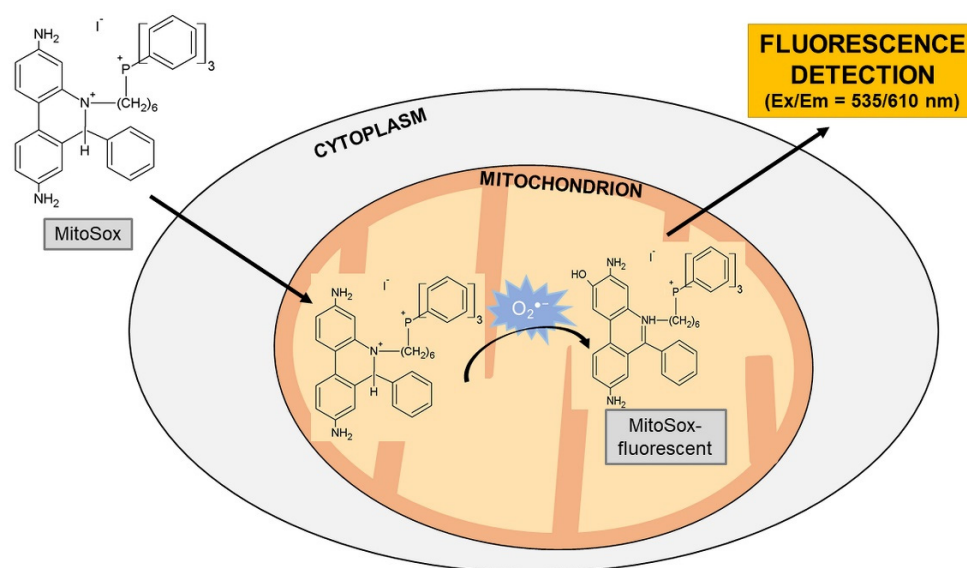


Figure 2. Detection of superoxide using MitoSox fluorescent probe. Abbreviation: O₂^{•−} = superoxide.

A new hydroethidine analog was synthesized for the purposes of O₂^{•−} detection, which is produced in mitochondria. This analog carries a charged triphenylphosphonium residue (Mito-HE; Mito-Sox Red). As the phosphonium residue is positively charged and surrounded by three lipophilic phenyl groups, it penetrates very easily through cell membranes, mainly through the inner mitochondrial membrane [72]. After they cross the cell membranes, they accumulate in mitochondria depending on the negative $\Delta\Psi$ [73]. Importantly, redistribution of MitoSox from mitochondria is dependent on decreasing

$\Delta\Psi$ based on various stimuli, which may not be ROS. For this reason, the use of MitoSox is a semi-quantitative test. Very important is the fact that MitoSox is transferred from mitochondria to the cytoplasm. Here, the supply of nucleic acids is higher and the increasing fluorescence is independent to mitochondrial ROS production, which may distort the results of individual measurements. The formation of MitoSox oxidation products in mitochondria may result in changes of values, which may reduce the passage of other MitoSox molecules into the mitochondria and generally affect measurements due to decreased MitoSox and ROS concentrations that are not produced by breathing chain breakage. The fluorescent product emits radiation at 580 nm with excitation at 540 nm [74–76].

1,3-Diphenylisobenzofuran

The 1,3-diphenylisobenzofuran (DPBF) probe is a molecule that, when incorporated into liposome phospholipids, acquires fluorescent properties. It is used for the detection of $O_2^{\bullet-}$ and 1O_2 . After reaction with oxygen radicals, it produces a decrease of fluorescence, thus the fluorescence rates correlate inversely with increasing concentrations of $O_2^{\bullet-}$ and 1O_2 [77,78]. The reaction of DPBF with ROS such as singlet oxygen, hydroxyl, alkoxy and alkyl peroxy radicals gives 1,2-dibenzoylbenzene. In contrast, only reaction with H_2O_2 produces 9-hydroxyanthracen-10-(9H)-one. This product can be detected using fluorescence spectroscopy, NMR spectroscopy, or HPLC [79].

2.2. Hydroxyl Radical

The hydroxyl radical is a neutral form of the hydroxide ion. It belongs among the most reactive ROS because it can react with a variety of organic and inorganic compounds including DNA, proteins, and lipids, resulting in serious cell damage. The hydroxyl radical may be formed as a product of the Fenton or Haber–Weiss reaction [80–83].

The Fenton reaction is based on the reaction between H_2O_2 and Fe^{2+} . Iron is an essential component of many proteins involved in the transport or metabolism of oxygen due to its ability to undergo cyclic oxidation and reduction. Iron has to be present for the ongoing synthesis of iron-containing proteins. As such, it can directly lead to the formation of free radicals, which can cause cellular damage of large extent. The reaction of Fe^{2+} with H_2O_2 produces an oxidized form of iron (Fe^{3+}), as well as $\bullet OH$ and OH^- (Equation (3)).



Another possible reaction to form $\bullet OH$ is the Haber–Weiss reaction. In this reaction, less reactive $O_2^{\bullet-}$ and H_2O_2 react with each other (Equation (4)). As in the case of the Fenton reaction, very toxic $\bullet OH$ is formed. Very unfavorable thermodynamic conditions are applied to this reaction, in which the rate constant in the aqueous solution is close to zero. The presence of a transition metal catalyst is required to ensure the reaction. The iron atom serves as the catalyst. Both reactions produce highly reactive $\bullet OH$, which ultimately severely damages cells [84–87]. The Fenton reaction can be used to induce apoptosis in cancer cells, where $\bullet OH$ is formed on a copper ion [88,89].

2.2.1. Role of Hydroxyl Radical in Nanomaterial Toxicity

TiO_2 and ZnO NPs are widely used in cosmetics and industry [22]. Under the influence of UV radiation, ZnO NPs generate reactive oxygen species such as $\bullet OH$ or H_2O_2 , causing GSH depletion [33,90]. The rate of $\bullet OH$ generation and the total photocatalytic activity depends on the physical properties of the nanomaterial used, e.g., TiO_2 NPs [34]. Cu NPs play an important role as a cofactor in a number of enzymes such as cytochrome c oxidase [91]. However, they exhibit significant toxicity and can induce ROS production, including largely reactive $\bullet OH$. Copper can catalyze electron transfer (Cu^{2+} and Cu^+). This can give rise to $O_2^{\bullet-}$ reduction to H_2O_2 in cells, leading to GSH depletion [35]. Other

particles that induce $\bullet\text{OH}$ production include Fe_3O_4 [92], silica nanoparticle [93], and silver nanoparticles [94].

2.2.2. Methods for the Detection of Hydroxyl Radical

Terephthalic acid (TA) can be hydroxylated in presence of $\bullet\text{OH}$ to give the highly fluorescent product 2-hydroxy-TA [95]. TA has a configuration of two carboxylate anion (COO^-) side groups attached to a six-carbon ring at positions 1 and 4 to form a structurally symmetrical compound. Reaction of $\bullet\text{OH}$ with any of the four unsubstituted carbons will form only one hydroxylated product, 2-hydroxy-TA (2-OH-TA). TA is non-fluorescent, whereas 2-OH-TA is highly fluorescent. Neither TA nor 2-OH-TA is present in tissues physiologically. In addition, none of them is known to be involved in cellular functions, thus they exhibit no cellular toxicity [96].

Fluorogenic spin probes can be used to detect $\bullet\text{OH}$. Their signal can be detected both fluorometrically and using EPR spectroscopy. The rhodamine nitroxide probe is a non-fluorescent substance reacting quantitatively with $\bullet\text{OH}$ ($E_x/E_m = 560/588 \text{ nm}$) [97].

The HKOH-1 probe was designed for better uptake and longer retention in cells. The HKOH-1 probe has excellent sensitivity, selectivity, and extremely rapid turn-on response toward $\bullet\text{OH}$ in live cells in both confocal imaging and flow cytometry experiments [98].

2.3. Singlet Oxygen

Singlet oxygen ($^1\text{O}_2$), the highest energy state of molecular oxygen, has been extensively studied to oxidize toxic persistent organic contaminants [99]. Singlet oxygen is a highly reactive form of oxygen. It is produced during photochemical reactions or even physiologically in the respiratory chain of mitochondria. In excitation, molecular oxygen is excited to the first state ($1\Delta_g$) and then to the higher excited state ($1\Sigma_g$). In the first excited state, O_2 has two counter-spin electrons in a π orbital, while in the second excited state, O_2 has one counter-spin electron in two π orbitals [100,101]. The first excited state is highly reactive. $1\Delta_g$ $^1\text{O}_2$ is also produced physiologically, e.g., in the activation of neutrophils and macrophages [102,103]. It is a highly potent oxidizing agent that can cause fatal damage of DNA [104] or cell death [105,106].

Singlet oxygen reacts with several biological molecules including DNA, RNA, lipids, sterols, and especially proteins [107]. Amino acid residues of proteins can react with $^1\text{O}_2$ by direct chemical reaction or physical quenching. Physical quenching causes de-excitation of the singlet state of oxygen proved in proteins through the interaction with tryptophan residues [108].

2.3.1. Role of Singlet Oxygen in Nanomaterial Toxicity

Reactive oxygen species are formed by the reaction of photoinduced binding electrons with oxygen molecules. After the release of photoinduced electrons, valence band holes are formed on the surface of TiO_2 NPs that cannot oxidize water [109]. Another type of ROS that occurs during photocatalytic reactions on the surface of TiO_2 NPs is $^1\text{O}_2$ (Figure 3) [41]. Nanomaterials that can induce singlet oxygen production also include Ag NPs [42]. Nanomaterials-bound generation of $^1\text{O}_2$ can be also used in the treatment of tumors [43]. An activatable system has been developed that enables tumor-specific $^1\text{O}_2$ generation, based on a Fenton-like reaction between linoleic acid hydroperoxide (LAHP), tethered on FeO NPs and Fe^{2+} ions released from FeO NPs under acidic pH conditions [43]. After increased production of $^1\text{O}_2$ in cells, the intracellular concentration of GSH decreases [110–112].

2.3.2. Methods for the Detection of Singlet Oxygen

The DPAX-1 fluorescent probe (9-[2-(3-carboxy-9,10-diphenyl)-anthryl]-6-hydroxy-3H-xanthen-3-one) has been used to detect $^1\text{O}_2$ forming endoperoxide as a reaction product. The probe is based on 9,10-diphenylanthracene (DPA), conjugated to fluorescein. The high quantum yield and wavelength of the excitation radiation are suitable for biological applications [113]. The DMAX 9-[2-(3-carboxy-9,10-dimethyl)anthryl]-6-hydroxy-3H-xanthen-3-

one has been also used to detect $^1\text{O}_2$. The DMAX probe reacts much more specifically and faster with $^1\text{O}_2$ compared to the DPAX-1 probe [114].

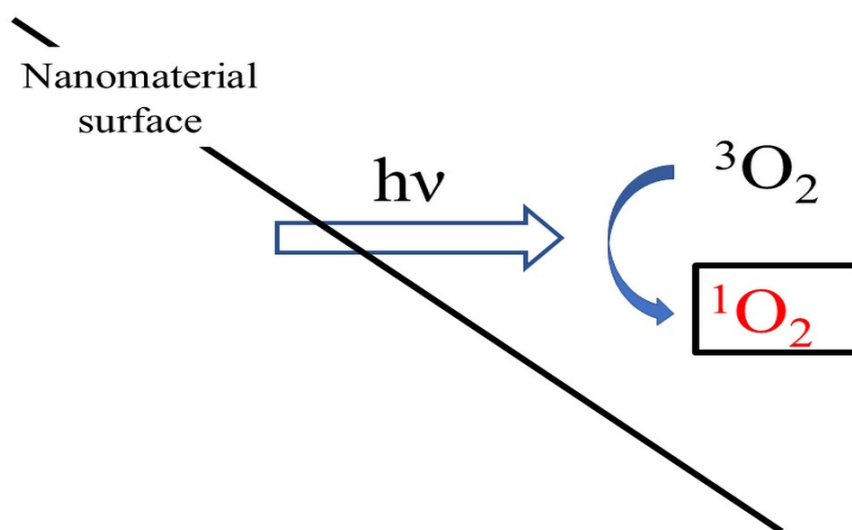


Figure 3. Generation of $^1\text{O}_2$ in a photocatalytic reaction on the TiO_2 surface. Abbreviations: $^3\text{O}_2$ = molecular oxygen; $^1\text{O}_2$ = singlet oxygen; and $h\nu$ = radiation.

Other approach for singlet oxygen detection are amino-functionalized nanoparticles covalently linked to Singlet Oxygen Sensor Green[®] (SOSG) which is an anthracene-fluorescein dye. The fluorescence of the SOSG molecule is inhibited by photoinduced intramolecular electron transfer. When anthracene is endoperoxidized in the presence of $^1\text{O}_2$, the electron transfer is blocked and fluorescein self-fluorescence is restored [115].

2.4. Hydrogen Peroxide

Hydrogen peroxide is formed directly through SOD-catalyzed dismutation from superoxide [116]. It belongs among ROS but it is not a free radical. The relatively long lifespan and size of H_2O_2 allows it to pass through cell membranes to different parts of the cell, which facilitates signaling reactions [117]. It causes cell damage at concentrations higher than 100 nM. Concentration of H_2O_2 in the range of 1–10 nM acts physiologically in the process of redox signaling [116]. It does not cause direct DNA damage but DNA damage is ensured due to $\bullet\text{OH}$ presence, which arises from H_2O_2 in the presence of transition metal ions [118]. Enzymes eliminating H_2O_2 include catalase, glutathione peroxidase, and peroxiredoxins [119].

In peroxisomes, the main metabolic process producing H_2O_2 is the β -oxidation of fatty acids through acyl-CoA-oxidase. Other enzymes involved in the formation of ROS include urate oxidase [120], D-aspartate oxidase [121], or xanthine oxidase [28].

2.4.1. Role of Hydrogen Peroxide in Nanomaterial Toxicity

Most nanomaterials that induce the production of $\text{O}_2^{\bullet-}$ also induce the production of H_2O_2 . In a study [36], colorectal cancer cells were exposed to polystyrene NPs (20 and 40 nm) with two surfactants (amino and carboxylic acid). After the exposure of cells to polystyrene NPs, a decrease in cell viability was observed and the induction of the apoptosis process was reduced by decreased H_2O_2 production by catalase. In another study [37], the authors observed a decrease in intracellular GSH concentration after the exposure of cells to 8 nm Au NPs. Subsequently, it was found that there was a decrease in mitochondrial membrane potential ($\Delta\Psi$) and cell apoptosis deepened after 48 h of incubation of cells with Au NPs. Then, a decreased mitochondrial GSH concentration and increased H_2O_2 production were observed. Other nanomaterials capable of induction of H_2O_2 formation are e.g., TiO_2 NPs [38], ZnO NPs [39], and Ag NPs [40].

2.4.2. Methods for the Detection of Hydrogen Peroxide

2',7'-Dichlorodihydrofluorescein

The 2',7'-dichlorodihydrofluorescein (DCFH) probe is a specific indicator of the presence of H_2O_2 . The diacetate form of DCFH (DCFH-DA) has been used to detect ROS in cells due to its ability to penetrate cell membranes. Two acetate groups are hydrolyzed by intracellular esterases after DCFH-DA transfer into cells. Then, the presence of peroxidases is important for the oxidation of DCFH by H_2O_2 . Other agents capable of oxidizing DCFH include hematin or cytochrome c [122,123] which may increase the fluorescence of the probe without any H_2O_2 production [124]. DCFH can be also oxidized with H_2O_2 in the presence of Fe^{2+} but this is most likely due to the formation of $\bullet\text{OH}$. In contrast, $\text{O}_2^{\bullet-}$ is unable to oxidize the DCFH probe [125]. In the presence of visible light or ultraviolet radiation, a DCF photoreduction can occur (Figure 4). The fluorescent product exhibits fluorescence at 522 nm (excitation at 498 nm).

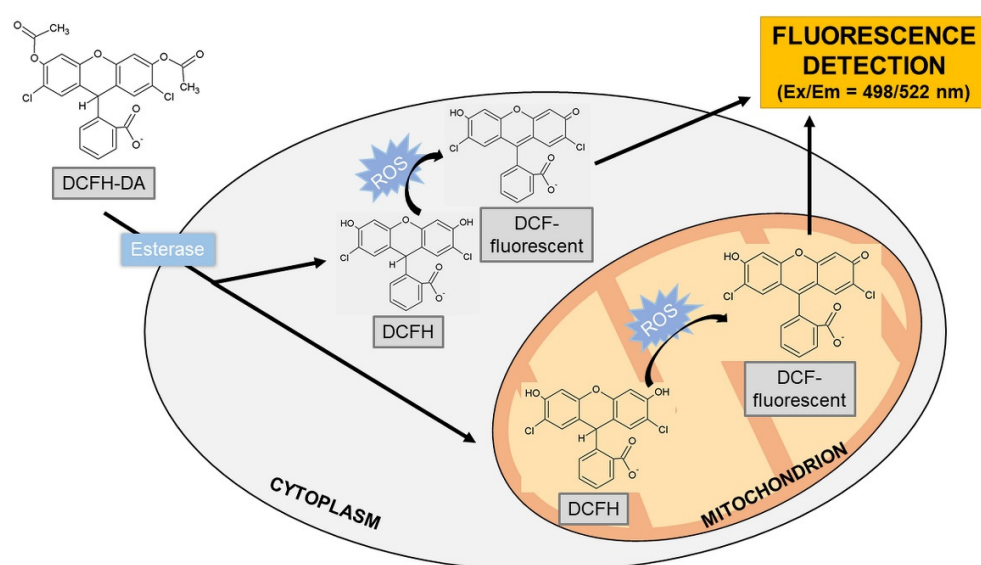


Figure 4. Detection of hydrogen peroxide using a probe DCFH-DA. Abbreviations: DCFH-DA = 2',7'-dichlorodihydrofluorescein diacetate; DCFH = 2',7'-dichlorodihydrofluorescein; DCF = 2',7'-dichlorofluorescein; and ROS = reactive oxygen species.

The oxidation of the probe produces a semichinone radical ($\text{DCF}^{\bullet-}$) that, when reacted with O_2 , gives rise to $\text{O}_2^{\bullet-}$. Dismutation of $\text{O}_2^{\bullet-}$ produces H_2O_2 that then artificially increases the oxidation of DCFH. The oxidation of DCFH results in the formation of a fluorescent product DCF exhibiting strong fluorescence. However, this reaction can increase the fluorescence intensity of the DCF product and give false-positive results [126–128]. In the case of the measurement of ROS production in tested nanomaterials, the form of DCFH-DA has been mostly used in ZnO_2 NMs [33,129–132] and TiO_2 NMs [133–136].

Amplex Red

Amplex Red (N-acetyl-3,7-dihydroxyphenoxazine) is a non-fluorescent molecule that can be specifically oxidized by H_2O_2 in the presence of horseradish peroxidase (HRP) to the highly fluorescent resorufin product (Figure 5), EX/EM 563/587 nm [137]. At excessive H_2O_2 concentrations, the fluorescent product resorufin can be further oxidized to non-fluorescent resazurin [138]. Amplex Red reacts with H_2O_2 stoichiometrically. It can also be used for the detection of $\text{O}_2^{\bullet-}$ in a mixture with SOD converting $\text{O}_2^{\bullet-}$ to H_2O_2 . The background fluorescence during the measurement is very low and the fluorescent product is very stable. These features increase the sensitivity of the measurement. Significant loss of fluorescence may be due to the oxidation of resorufin to the non-fluorescent resazurin product that can be catalyzed by HRP [139,140].

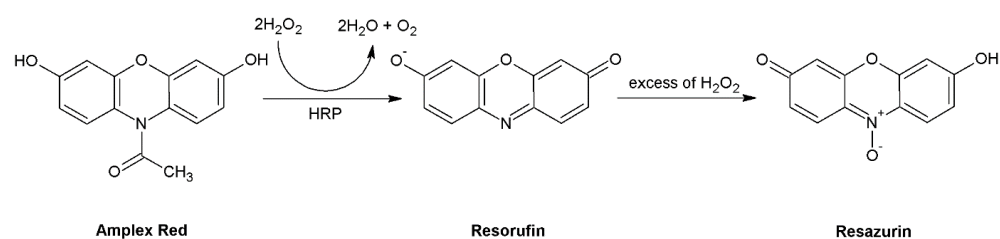


Figure 5. Oxidation of Amplex Red to a fluorescent (resorufin) and non-fluorescent (resazurin) product. Abbreviation: HRP = horseradish peroxidase.

HyPer Ratiometric Sensor

The H_2O_2 concentration can be measured using the expression of a HyPer genetically encoded ratio sensor. HyPer consists of the bacterial H_2O_2 -sensitive transcription factor OxyR, fused to the circular fluorescent protein YFP. Cysteine oxidation of the OxyR moiety induces a conformational change that results in an increase in YFP fluorescence intensity excited at 500 nm and a decrease in YFP emission excited at 420 nm. This reversible change can monitor the intracellular concentration of H_2O_2 [141].

Pentafluorobenzenesulfonyl Fluoresceins

Perhydrolysis of acyl resorufins is a reaction that acts as a fluorescent indicator for the determination of H_2O_2 . This method is based on deprotection rather than oxidation, which enables the fluorescence of resorufin and fluorescein. The selectivity of this method for H_2O_2 detection is higher compared to DCFH. For the above reasons, pentafluorobenzenesulfonyl fluoresceins have been proposed as selective fluorescent probes for H_2O_2 detection. Importantly, sulfonates are more stable to hydrolysis than esters. Fluoresceins have high fluorescence yields and the pentafluorobenzene ring increases the reactivity of sulfonates with H_2O_2 [142].

Europium Ion

The method is based on the binding of Eu^{3+} -tetracycline [Eu (tc)] linked to propane-sulfonic acid (MOPS) in an aqueous solution to H_2O_2 . After binding, a strongly fluorescent complex ([Eu (hp) (tc)]) is formed ($\lambda_{\text{EX/EM}} = 390\text{-}405 / 616 \text{ nm}$). The increase in fluorescence is up to 15x after H_2O_2 binding and it is strongly dependent on the pH value. The increase in fluorescence is most pronounced at the physiological pH environment. The fluorescence of the probe [Eu (tc)] is not affected by ammonium, chloride, sulphate, or nitrate ions. However, citrate and phosphate can interfere with the assay [143].

Homovanillic Acid

Recently, homovanillic acid (3-methoxy-4-hydroxyphenylacetic acid) has been increasingly used instead of scopoletin for H_2O_2 detection in mitochondria. In contrast to the fluorescent scopoletin indicating the presence of H_2O_2 by a fluorescence decrease, homovanillic acid becomes a fluorescent through H_2O_2 -induced oxidation in the presence of HRP [144]. The product of this reaction is a highly fluorescent dimer 2,2'-dihydroxy-3,3'-dimethoxydiphenyl-5,5'-diacetic acid [145]. In the following Table 2, an overview of all described fluorescent probes for ROS detection are summarized.

Table 2. Overview of fluorescent probes for the detection of ROS [79,95,97,98,114,115,137,141–143,145].

Type of ROS	Fluorescent Probe	Excitation/Emission Wavelengths
Superoxide	MitoSox	535/610 nm
	1,3-diphenylisobenzofuran	410/455 nm
Hydroxyl radical	Terephthalic acid	310/420 nm
	Rhodamine nitroxide	560/588 nm
	HKOH-1	500/520 nm
Singlet oxygen	DPAX-1	495/515 nm
	DMAX	495/515 nm
	Singlet Oxygen Sensor Green®	504/525 nm
Hydrogen peroxide	2',7'-dichlorodihydrofluorescein	498/522 nm
	Amplex Red	563/587 nm
	HyPer ratiometric sensor	485/516 nm
	Pentafluorobenzenesulfonyl fluoresceins	485/530 nm
	Europium ion	400/616 nm
	Homovanilic acid	312/420 nm

3. Role of Reactive Oxygen Species Induced by Nanoparticles in Cell Signaling

Nanomaterials are capable of interfering with cell signaling pathways. Recently, three main pathways participating in the apoptosis process have been identified (Figure 6). The first pathway is the direct NMs occupation of the FADD receptor. The second pathway is the modulation of the function of mitochondria in the presence of NMs and the third is the localization of NMs pacting in the endoplasmic reticulum. All of these pathways converge upon caspase activation, thereby the mitochondria produce higher levels of ROS, increase production of Bid protein, and activate Bax or Bak1 proteins, which can ultimately lead to organelle damage, DNA cleavage, and cell death [146].

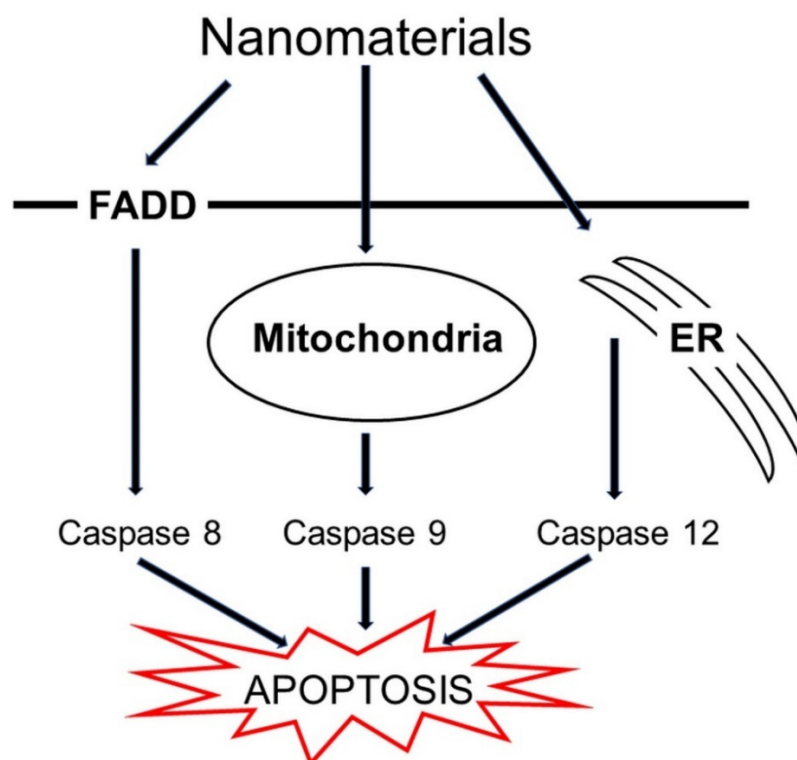


Figure 6. Possible pathways of induction of apoptosis by nanomaterials in cells. Abbreviations: ER = endoplasmic reticulum and FADD = FAS-associated death domain protein.

The dynamic and rapid nature of ROS signaling is the result of ROS production and removal. The balance between the production and removal of ROS is balanced due to their interaction. This causes rapid changes in ROS levels [147]. ROS play an important role in activating many cellular proteins and factors, e.g., NF- κ B, MAPK, Keap1-Nrf2-ARE, or PI3K-Akt [148,149].

The NF- κ B family is a family of transcriptional proteins consisting of five members, i.e., NF- κ B1, NF- κ B2, RelA, RelB, and c-Rel [150]. The activation of the transcription factor NF- κ B involves signal-dependent degradation of phosphorylated inhibitors such as I κ B α . The mechanism of NF- κ B activation by H₂O₂ [151] or O₂^{•-} [152] is different from the activation in the presence of cytokines or mitogens. Serines 32 and 36 play a key role in the activation of NF- κ B by cytokines, while tyrosine residues 42 and serine/threonine in the PEST domain of the I κ B α protein play a key role in the activation by H₂O₂ [153]. H₂O₂ activates I κ B α kinase without subsequent serine phosphorylation of I κ B α . In contrast, H₂O₂, similar to TNF, induces serine phosphorylation of the p65 subunit of NF- κ B, leading to its nuclear translocation [154]. Nanoparticles participate directly in the activation of the factor NF- κ B through increased ROS production which was confirmed by the translocation of the high-mobility group box 1 (HMGB1) protein from the nucleus to the cytoplasm observed in cells after exposure to silica nanoparticles [155]. Subsequently, HMGB1 binds to the TLR4 receptor; this complex regulates the expression of the myeloid differentiation factor and activates the NF- κ B-signaling pathway.

In eukaryotic cells, signaling by MAPK kinases is very important. Various MAPK pathways can be activated by different stimuli. Ultimately, activated MAPK pathways coordinate gene transcription activation, acting in the regulation of protein synthesis, cell cycle, cell death, and cell differentiation [156]. The MAPK cascade is composed of three distinct signaling modules, i.e., the c-Jun N-terminal kinase cascade, the p38 MAPK cascade, and the extracellular signal-regulated kinase ERK [157]. Several cellular stimuli activating ROS production can also activate MAPK activation itself [158]. For instance, MAPK kinases can be activated by H₂O₂ [159]. MAPK activation occurs by activating growth factor receptors in several cell types [160]. Another mechanism of MAPK activation by ROS is the inactivation of the MKP protein by its oxidation [161]. The physiological FEM protein keeps the MAPK signaling pathway inactive. In addition to the activation of MAPK, the JNK pathway is also activated during the oxidation of the FEM protein [162]. A number of studies have demonstrated the activation of a variety of kinases by ROS, including ASK1 [163], MEKK1 [164], c-Src [165], and EGFR [166]. These activated kinases ultimately can activate the MAPK cascade [167]. Cerium oxide particles have been shown to activate ROS production and to reduce SOD and glutathione peroxidase activities. This results in increased phosphorylation levels of p38 MAPK as well as ERK1/2 and JNK [168]. The nanoparticles that can damage cells through p38 MAPK activation are silica NPs [169,170], polystyrene NPs [171], and TiO₂ NPs [172]. Conversely, the exposure to Au [173] and iron oxide [174] NPs causes the osteogenic differentiation through the activation of relevant genes by p38 MAPK.

The tumor suppressor protein p53 induces apoptotic cell death in response to oncogenic stress. Malignant progression is dependent on the loss of p53 function by mutations in the TP53 gene itself or defects in signaling pathways. Phosphorylation of p53 regulates the ability to activate the expression of apoptotic target genes [175]. Overexpression of p53 transactivates a number of p53 genes. Many of these genes encode redox active proteins including enzymes (quinone oxidoreductase and proline oxidase) generating ROS. Ultimately, this regulation of ROS production leads to oxidative stress that can induce apoptosis [176]. Increasing the intracellular concentration of ROS leads to the activation of the p38 protein, which increases the expression and transcriptional activity of p53 [177]. The p53 protein transcriptionally activates the PUMA gene encoding two proteins, PUMA- α and PUMA- β , of similar activity. These proteins bind to Bcl-2 and integrate into the mitochondria, where they induce the release of cytochrome c [178–180].

Last but not least, ROS activate the JNK kinase pathway, which plays an important role in the apoptosis process [4,181]. During intracellular ROS production, there is a permanent activation of JNK [182]. This is due to the inactivation of MAPK phosphatases (FEM) by oxidation of their catalytic cysteine in the presence of intracellularly accumulated H_2O_2 . Expression of catalytically inactive FEMs prolongs JNK activation [183].

4. Current Trends in the Evaluation of Nanotoxicity In Vitro

The number of studies focusing on nanotoxicity testing has been growing very rapidly in the last two decades. The cause of that can be also found in the perpetual production of new nanomaterials for its following use in industry or medicine. Conversely, especially in medicine, nanomaterials raise some concerns regarding their cytotoxicity or biocompatibility. Thus, a number of scientific projects have been assessing the toxicity of the selected nanomaterials and creating the risk management framework for the use of nanomaterials in medical applications [184].

Recent studies on nanotoxicity have been using basic assays for the evaluation of cell function changes, e.g., cell viability, membrane integrity, and enzyme activities measurements. To estimate the oxidative status in cells, the levels of antioxidants can be measured using a number of methods. In addition to the most frequently used methods, other approaches have been used to characterize the cellular nanotoxicity recently. These methods include scanning electron microscopy [185], liquid cell transmission electron microscopy [186], atomic force microscopy [187], and hyperspectral and laser confocal microscopy applied to cell-nanoparticles interactions [185]. All these microscopic methods are very sensitive and specific, which allows for a very detailed description of the function state of the cells after nanomaterials treatment. To understand the toxicity of nanomaterials, we need to develop new and innovative methods that will provide us with information about the changes in the intracellular environment after exposure to nanomaterials. In addition, there is a need to develop methods that are fast, robust, and combine several biological tests. In contrast to conventional assays using lipophilic fluorescent probes detecting ROS levels, a nanoelectrode has been developed to study the toxicity of magnetic nanoparticles. The nanoelectrode is composed of individual platinum nanoelectrodes with a cavity at the tip. It is part of an upright microscope and is used to measure intracellular ROS [188].

A further topic of interest in nanotoxicity testing is the use of newly developed relevant biological models. In comparison to two-dimensional (2D) cultured cell lines, those new biological models ought to provide accurate predictions of nanomaterials effects in vivo. Thus, some new scientific studies described the use of pulmonary fibrosis models [189], organ on-chip technology bridging the differences between 2D in vitro and three-dimensional (3D) in vivo models from skin, the lung, and the liver [190,191], or on-chip placenta models [192]. Despite advanced organ on-chip models, a number of concerns have to be solved to ensure the comparability to living systems in obtained outcomes [193].

5. Conclusions

Currently, nanotechnology is considered to be one of the most attractive research topics due to its huge application potential and commercial impact. Due to the large number of newly manufactured nanomaterials, it is necessary to evaluate their possible cytotoxic effects in men. At present, there is a large request to investigate the potential acute and chronic effects of nanomaterials especially in vitro in cells. Those studies can provide a mechanistic view on nanomaterial cellular acting. However, the use of proper and relevant bioanalytical methods for evaluating the nanomaterials effects in cells is necessary.

In this study, we aimed to provide a recent and detailed view on ROS production induced by nanomaterials, especially considering the metallic nanoparticles. In cells, the nanotoxicity can be mediated by a number of substances including ROS. Depending on the composition and shape of a nanomaterial, a variety of ROS can be formed in cells, i.e., $O_2^{\bullet-}$, 1O_2 , $\bullet OH$, and H_2O_2 . Thus, the importance of the present review can

be recognized in the mechanistic description of a relation of nanomaterials of different chemical compositions and ROS production. We provided the current knowledge of ROS-mediated cellular nanotoxicity together with the possibilities of ROS detection in cells using specific fluorescent probes. In addition, we summarized the detailed description of the relationship between nanomaterials-mediated ROS production and glutathione depletion. Altogether, the prooxidative action of nanomaterials can ultimately lead to the activation of cellular signaling pathways, causing a change in cellular metabolism, cell damage, or even cell death.

Funding: Financial support was received from the Ministry of Education, Youth, and Sports of the Czech Republic via project NANOBIO (Reg. No. CZ.02.1.01/0.0/0.0/17_048/0007421).

Institutional Review Board Statement: Not applicable.

Informed Consent Statement: Not applicable.

Data Availability Statement: Not applicable.

Conflicts of Interest: The authors declare no conflict of interest.

References

1. Hayyan, M.; Hashim, M.A.; AlNashef, I.M. Superoxide Ion: Generation and Chemical Implications. *Chem. Rev.* **2016**, *116*, 3029–3085. [[CrossRef](#)] [[PubMed](#)]
2. Lushchak, V.I. Free radicals, reactive oxygen species, oxidative stress and its classification. *Chem. Biol. Interact.* **2014**, *224*, 164–175. [[CrossRef](#)] [[PubMed](#)]
3. Juan, C.A.; Perez de la Lastra, J.M.; Plou, F.J.; Perez-Lebena, E. The Chemistry of Reactive Oxygen Species (ROS) Revisited: Outlining Their Role in Biological Macromolecules (DNA, Lipids and Proteins) and Induced Pathologies. *Int. J. Mol. Sci.* **2021**, *22*, 4642. [[CrossRef](#)] [[PubMed](#)]
4. Simon, H.U.; Haj-Yehia, A.; Levi-Schaffer, F. Role of reactive oxygen species (ROS) in apoptosis induction. *Apoptosis* **2000**, *5*, 415–418. [[CrossRef](#)] [[PubMed](#)]
5. Wagner, H.; Cheng, J.W.; Ko, E.Y. Role of reactive oxygen species in male infertility: An updated review of literature. *Arab. J. Urol.* **2018**, *16*, 35–43. [[CrossRef](#)] [[PubMed](#)]
6. Ott, M.; Gogvadze, V.; Orrenius, S.; Zhivotovsky, B. Mitochondria, oxidative stress and cell death. *Apoptosis* **2007**, *12*, 913–922. [[CrossRef](#)] [[PubMed](#)]
7. Zhao, R.Z.; Jiang, S.; Zhang, L.; Yu, Z.B. Mitochondrial electron transport chain, ROS generation and uncoupling (Review). *Int. J. Mol. Med.* **2019**, *44*, 3–15. [[CrossRef](#)] [[PubMed](#)]
8. Suski, J.; Lebiecinska, M.; Bonora, M.; Pinton, P.; Duszynski, J.; Wieckowski, M.R. Relation Between Mitochondrial Membrane Potential and ROS Formation. *Methods Mol. Biol.* **2018**, *1782*, 357–381. [[PubMed](#)]
9. Mazat, J.P.; Devin, A.; Ransac, S. Modelling mitochondrial ROS production by the respiratory chain. *Cell Mol. Life Sci.* **2020**, *77*, 455–465. [[CrossRef](#)] [[PubMed](#)]
10. Parey, K.; Wirth, C.; Vonck, J.; Zickermann, V. Respiratory complex I—structure, mechanism and evolution. *Curr. Opin. Struct. Biol.* **2020**, *63*, 1–9. [[CrossRef](#)]
11. Husen, P.; Nielsen, C.; Martino, C.F.; Solov'yov, I.A. Molecular Oxygen Binding in the Mitochondrial Electron Transfer Flavoprotein. *J. Chem. Inf. Model.* **2019**, *59*, 4868–4879. [[CrossRef](#)] [[PubMed](#)]
12. Mailloux, R.J. An Update on Mitochondrial Reactive Oxygen Species Production. *Antioxidants* **2020**, *9*, 472. [[CrossRef](#)] [[PubMed](#)]
13. Papa, S.; Skulachev, V.P. Reactive oxygen species, mitochondria, apoptosis and aging. *Mol. Cell Biochem.* **1997**, *174*, 305–319. [[CrossRef](#)] [[PubMed](#)]
14. Ventura, J.J.; Cogswell, P.; Flavell, R.A.; Baldwin, A.S., Jr.; Davis, R.J. JNK potentiates TNF-stimulated necrosis by increasing the production of cytotoxic reactive oxygen species. *Genes Dev.* **2004**, *18*, 2905–2915. [[CrossRef](#)] [[PubMed](#)]
15. Zhang, M.; Harashima, N.; Moritani, T.; Huang, W.; Harada, M. The Roles of ROS and Caspases in TRAIL-Induced Apoptosis and Necroptosis in Human Pancreatic Cancer Cells. *PLoS ONE* **2015**, *10*, e0127386. [[CrossRef](#)] [[PubMed](#)]
16. Yang, J.; Zhao, X.; Tang, M.; Li, L.; Lei, Y.; Cheng, P.; Guo, W.; Zheng, Y.; Wang, W.; Luo, N.; et al. The role of ROS and subsequent DNA-damage response in PUMA-induced apoptosis of ovarian cancer cells. *Oncotarget* **2017**, *8*, 23492–23506. [[CrossRef](#)] [[PubMed](#)]
17. Liou, G.Y.; Storz, P. Reactive oxygen species in cancer. *Free Radic. Res.* **2010**, *44*, 479–496. [[CrossRef](#)]
18. Storz, P. Reactive oxygen species in tumor progression. *Front. BioSci.* **2005**, *10*, 1881–1896. [[CrossRef](#)]
19. Zhou, B.; Guo, X.; Yang, N.; Huang, Z.; Huang, L.; Fang, Z.; Zhang, C.; Li, L.; Yu, C. Surface engineering strategies of gold nanomaterials and their applications in biomedicine and detection. *J. Mater. Chem. B* **2021**, *9*, 5583–5598. [[CrossRef](#)]
20. Sakr, T.M.; Korany, M.; Katti, K.V. Selenium nanomaterials in biomedicine—An overview of new opportunities in nanomedicine of selenium. *J. Drug Deliv. Sci. Technol.* **2018**, *46*, 223–233. [[CrossRef](#)]

21. Mehlenbacher, R.D.; Kolbl, R.; Lay, A.; Dionne, J.A. Nanomaterials for in vivo imaging of mechanical forces and electrical fields. *Nat. Rev. Mater.* **2017**, *3*, 1–17. [[CrossRef](#)]
22. Musial, J.; Krakowiak, R.; Mlynarczyk, D.T.; Goslinski, T.; Stanisz, B.J. Titanium Dioxide Nanoparticles in Food and Personal Care Products—What Do We Know about Their Safety? *Nanomaterials* **2020**, *10*, 1110. [[CrossRef](#)]
23. Holmila, R.J.; Vance, S.A.; King, S.B.; Tsang, A.W.; Singh, R.; Furdui, C.M. Silver Nanoparticles Induce Mitochondrial Protein Oxidation in Lung Cells Impacting Cell Cycle and Proliferation. *Antioxidants* **2019**, *8*, 552. [[CrossRef](#)] [[PubMed](#)]
24. Drasler, B.; Sayre, P.; Steinhäuser, K.G.; Petri-Fink, A.; Rothen-Rutishauser, B. In vitro approaches to assess the hazard of nanomaterials. *NanoImpact* **2017**, *8*, 99–116. [[CrossRef](#)]
25. Yin, J.J.; Liu, J.; Ehrenshaft, M.; Roberts, J.E.; Fu, P.P.; Mason, R.P.; Zhao, B. Phototoxicity of nano titanium dioxides in HaCaT keratinocytes—generation of reactive oxygen species and cell damage. *Toxicol. Appl. Pharmacol.* **2012**, *263*, 81–88. [[CrossRef](#)]
26. Ray, P.C.; Yu, H.T.; Fu, P.P. Toxicity and Environmental Risks of Nanomaterials: Challenges and Future Needs. *J. Environ. Sci. Health C* **2009**, *27*, 1–35. [[CrossRef](#)]
27. Daimon, T.; Nosaka, Y. Formation and behavior of singlet molecular oxygen in TiO₂ photocatalysis studied by detection of near-infrared phosphorescence. *J. Phys. Chem. C* **2007**, *111*, 4420–4424. [[CrossRef](#)]
28. Phaniendra, A.; Jestadi, D.B.; Periyasamy, L. Free Radicals: Properties, Sources, Targets, and Their Implication in Various Diseases. *Indian J. Clin. Biochem.* **2015**, *30*, 11–26. [[CrossRef](#)] [[PubMed](#)]
29. Yang, H.; Liu, C.; Yang, D.; Zhang, H.; Xi, Z. Comparative study of cytotoxicity, oxidative stress and genotoxicity induced by four typical nanomaterials: The role of particle size, shape and composition. *J. Appl. Toxicol.* **2009**, *29*, 69–78. [[CrossRef](#)]
30. He, X.; Sanders, S.; Aker, W.G.; Lin, Y.; Douglas, J.; Hwang, H.M. Assessing the effects of surface-bound humic acid on the phototoxicity of anatase and rutile TiO₂ nanoparticles in vitro. *J. Environ. Sci.* **2016**, *42*, 50–60. [[CrossRef](#)] [[PubMed](#)]
31. Zhang, J.; Wang, B.; Wang, H.; He, H.; Wu, Q.; Qin, X.; Yang, X.; Chen, L.; Xu, G.; Yuan, Z.; et al. Disruption of the superoxide anions-mitophagy regulation axis mediates copper oxide nanoparticles-induced vascular endothelial cell death. *Free Radic. Biol. Med.* **2018**, *129*, 268–278. [[CrossRef](#)] [[PubMed](#)]
32. Onodera, A.; Nishiumi, F.; Kakiguchi, K.; Tanaka, A.; Tanabe, N.; Honma, A.; Yayama, K.; Yoshioka, Y.; Nakahira, K.; Yonemura, S.; et al. Short-term changes in intracellular ROS localisation after the silver nanoparticles exposure depending on particle size. *Toxicol. Rep.* **2015**, *2*, 574–579. [[CrossRef](#)]
33. Ahamed, M.; Akhtar, M.J.; Raja, M.; Ahmad, I.; Siddiqui, M.K.; AlSalhi, M.S.; Alrokayan, S.A. ZnO nanorod-induced apoptosis in human alveolar adenocarcinoma cells via p53, survivin and bax/bcl-2 pathways: Role of oxidative stress. *Nanomedicine* **2011**, *7*, 904–913. [[CrossRef](#)] [[PubMed](#)]
34. Jimenez-Relinque, E.; Castellote, M. Hydroxyl radical and free and shallowly trapped electron generation and electron/hole recombination rates in TiO₂ photocatalysis using different combinations of anatase and rutile. *Appl. Catal. A Gen.* **2018**, *565*, 20–25. [[CrossRef](#)]
35. Thit, A.; Selck, H.; Bjerregaard, H.F. Toxic mechanisms of copper oxide nanoparticles in epithelial kidney cells. *Toxicol. In Vitro* **2015**, *29*, 1053–1059. [[CrossRef](#)]
36. Thubagere, A.; Reinhard, B.M. Nanoparticle-induced apoptosis propagates through hydrogen-peroxide-mediated bystander killing: Insights from a human intestinal epithelium in vitro model. *ACS Nano* **2010**, *4*, 3611–3622. [[CrossRef](#)]
37. Gao, W.; Xu, K.; Ji, L.; Tang, B. Effect of gold nanoparticles on glutathione depletion-induced hydrogen peroxide generation and apoptosis in HL7702 cells. *Toxicol. Lett.* **2011**, *205*, 86–95. [[CrossRef](#)] [[PubMed](#)]
38. Wang, J.X.; Fan, Y.B.; Gao, Y.; Hu, Q.H.; Wang, T.C. TiO₂ nanoparticles translocation and potential toxicological effect in rats after intrarticular injection. *Biomaterials* **2009**, *30*, 4590–4600. [[CrossRef](#)] [[PubMed](#)]
39. Guo, D.; Bi, H.; Liu, B.; Wu, Q.; Wang, D.; Cui, Y. Reactive oxygen species-induced cytotoxic effects of zinc oxide nanoparticles in rat retinal ganglion cells. *Toxicol. In Vitro* **2013**, *27*, 731–738. [[CrossRef](#)]
40. Yang, E.J.; Kim, S.; Kim, J.S.; Choi, I.H. Inflammasome formation and IL-1 β release by human blood monocytes in response to silver nanoparticles. *Biomaterials* **2012**, *33*, 6858–6867. [[CrossRef](#)] [[PubMed](#)]
41. Hirakawa, K.; Hirano, T. Singlet oxygen generation photocatalyzed by TiO₂ particles and its contribution to biomolecule damage. *Chem. Lett.* **2006**, *35*, 832–833. [[CrossRef](#)]
42. Lee, S.H.; Jun, B.H. Silver Nanoparticles: Synthesis and Application for Nanomedicine. *Int. J. Mol. Sci.* **2019**, *20*, 865. [[CrossRef](#)] [[PubMed](#)]
43. Zhou, Z.; Song, J.; Tian, R.; Yang, Z.; Yu, G.; Lin, L.; Zhang, G.; Fan, W.; Zhang, F.; Niu, G.; et al. Activatable Singlet Oxygen Generation from Lipid Hydroperoxide Nanoparticles for Cancer Therapy. *Angew. Chem. Int. Ed. Engl.* **2017**, *56*, 6492–6496. [[CrossRef](#)]
44. Abdal Dayem, A.; Hossain, M.K.; Lee, S.B.; Kim, K.; Saha, S.K.; Yang, G.M.; Choi, H.Y.; Cho, S.G. The Role of Reactive Oxygen Species (ROS) in the Biological Activities of Metallic Nanoparticles. *Int. J. Mol. Sci.* **2017**, *18*, 120. [[CrossRef](#)]
45. Kermanizadeh, A.; Jantzen, K.; Ward, M.B.; Durhuus, J.A.; Juel Rasmussen, L.; Loft, S.; Moller, P. Nanomaterial-induced cell death in pulmonary and hepatic cells following exposure to three different metallic materials: The role of autophagy and apoptosis. *Nanotoxicology* **2017**, *11*, 184–200. [[CrossRef](#)] [[PubMed](#)]
46. Ge, D.; Du, Q.; Ran, B.; Liu, X.; Wang, X.; Ma, X.; Cheng, F.; Sun, B. The neurotoxicity induced by engineered nanomaterials. *Int. J. Nanomed.* **2019**, *14*, 4167–4186. [[CrossRef](#)] [[PubMed](#)]
47. Fridovich, I. Biological effects of the superoxide radical. *Arch. BioChem. Biophys.* **1986**, *247*, 1–11. [[CrossRef](#)]

48. Apel, K.; Hirt, H. Reactive oxygen species: Metabolism, oxidative stress, and signal transduction. *Annu. Rev. Plant. Biol.* **2004**, *55*, 373–399. [[CrossRef](#)]
49. McIntyre, M.; Bohr, D.F.; Dominiczak, A.F. Endothelial function in hypertension: The role of superoxide anion. *Hypertension* **1999**, *34*, 539–545. [[CrossRef](#)]
50. Bielski, B.H.J.; Cabelli, D.E. Superoxide and Hydroxyl Radical Chemistry in Aqueous Solution. *Act. Oxyg. Chem.* **1995**, *2*, 66–104.
51. Ahsan, H.; Ali, A.; Ali, R. Oxygen free radicals and systemic autoimmunity. *Clin. Exp. Immunol.* **2003**, *131*, 398–404. [[CrossRef](#)]
52. Perry, J.J.P.; Shin, D.S.; Getzoff, E.D.; Tainer, J.A. The structural biochemistry of the superoxide dismutases. *Bba-Proteins Proteom.* **2010**, *1804*, 245–262. [[CrossRef](#)]
53. Borgstahl, G.E.O.; Oberley-Deegan, R.E. Superoxide Dismutases (SODs) and SOD Mimetics. *Antioxidants* **2018**, *7*, 156. [[CrossRef](#)]
54. Landis, G.N.; Tower, J. Superoxide dismutase evolution and life span regulation. *Mech. Ageing Dev.* **2005**, *126*, 365–379. [[CrossRef](#)] [[PubMed](#)]
55. Loschen, G.; Flohe, L.; Chance, B. Respiratory Chain Linked H₂O₂ Production in Pigeon Heart Mitochondria. *FEBS Lett.* **1971**, *18*, 261–264. [[CrossRef](#)]
56. Loschen, G.; Azzi, A.; Richter, C.; Flohe, L. Superoxide Radicals as Precursors of Mitochondrial Hydrogen-Peroxide. *FEBS Lett.* **1974**, *42*, 68–72. [[CrossRef](#)]
57. Wilson, D.F.; Erecinska, M.; Dutton, P.L. Thermodynamic Relationships in Mitochondrial Oxidative-Phosphorylation. *Annu. Rev. Biophys. Bio* **1974**, *3*, 203–230. [[CrossRef](#)] [[PubMed](#)]
58. Ballard, J.W.; Youngson, N.A. Review: Can diet influence the selective advantage of mitochondrial DNA haplotypes? *Biosci. Rep.* **2015**, *35*. [[CrossRef](#)] [[PubMed](#)]
59. Liu, Y.B.; Fiskum, G.; Schubert, D. Generation of reactive oxygen species by the mitochondrial electron transport chain. *J. NeuroChem.* **2002**, *80*, 780–787. [[CrossRef](#)] [[PubMed](#)]
60. Kushnareva, Y.; Murphy, A.N.; Andreyev, A. Complex I-mediated reactive oxygen species generation: Modulation by cytochrome c and NAD(P)⁺ oxidation-reduction state. *Biochem. J.* **2002**, *368*, 545–553. [[CrossRef](#)]
61. Murphy, M.P. How mitochondria produce reactive oxygen species. *Biochem. J.* **2009**, *417*, 1–13. [[CrossRef](#)] [[PubMed](#)]
62. Wikstrom, M.K.; Berden, J.A. Oxidoreduction of cytochrome b in the presence of antimycin. *Biochim. Biophys. Acta* **1972**, *283*, 403–420. [[CrossRef](#)]
63. Muller, F.; Crofts, A.R.; Kramer, D.M. Multiple Q-cycle bypass reactions at the Q_o site of the cytochrome *bc*₁ complex. *Biochemistry* **2002**, *41*, 7866–7874. [[CrossRef](#)] [[PubMed](#)]
64. Bleier, L.; Drose, S. Superoxide generation by complex III: From mechanistic rationales to functional consequences. *Biochim. Biophys. Acta* **2013**, *1827*, 1320–1331. [[CrossRef](#)] [[PubMed](#)]
65. Grzelak, A.; Wojewodzka, M.; Meczynska-Wielgosz, S.; Zuberek, M.; Wojciechowska, D.; Kruszewski, M. Crucial role of chelatable iron in silver nanoparticles induced DNA damage and cytotoxicity. *Redox Biol.* **2018**, *15*, 435–440. [[CrossRef](#)] [[PubMed](#)]
66. Jayaram, D.T.; Payne, C.K. Intracellular Generation of Superoxide by TiO₂ Nanoparticles Decreases Histone Deacetylase 9 (HDAC9), an Epigenetic Modifier. *Bioconjug. Chem.* **2020**, *31*, 1354–1361. [[CrossRef](#)]
67. Masoud, R.; Bizouarn, T.; Trepout, S.; Wien, F.; Baciou, L.; Marco, S.; Houee Levin, C. Titanium Dioxide Nanoparticles Increase Superoxide Anion Production by Acting on NADPH Oxidase. *PLoS ONE* **2015**, *10*, e0144829. [[CrossRef](#)]
68. Akhtar, M.J.; Kumar, S.; Alhadlaq, H.A.; Alrokayan, S.A.; Abu-Salah, K.M.; Ahamed, M. Dose-dependent genotoxicity of copper oxide nanoparticles stimulated by reactive oxygen species in human lung epithelial cells. *Toxicol. Ind. Health* **2016**, *32*, 809–821. [[CrossRef](#)] [[PubMed](#)]
69. Piret, J.P.; Jacques, D.; Audinot, J.N.; Mejia, J.; Boilan, E.; Noel, F.; Fransolet, M.; Demazy, C.; Lucas, S.; Saout, C.; et al. Copper (II) oxide nanoparticles penetrate into HepG2 cells, exert cytotoxicity via oxidative stress and induce pro-inflammatory response. *Nanoscale* **2012**, *4*, 7168–7184. [[CrossRef](#)]
70. Piao, M.J.; Kang, K.A.; Lee, I.K.; Kim, H.S.; Kim, S.; Choi, J.Y.; Choi, J.; Hyun, J.W. Silver nanoparticles induce oxidative cell damage in human liver cells through inhibition of reduced glutathione and induction of mitochondria-involved apoptosis. *Toxicol. Lett.* **2011**, *201*, 92–100. [[CrossRef](#)] [[PubMed](#)]
71. Zielonka, J.; Srinivasan, S.; Hardy, M.; Ouari, O.; Lopez, M.; Vasquez-Vivar, J.; Avadhani, N.G.; Kalyanaraman, B. Cytochrome c-mediated oxidation of hydroethidine and mito-hydroethidine in mitochondria: Identification of homo- and heterodimers. *Free Radic. Biol. Med.* **2008**, *44*, 835–846. [[CrossRef](#)] [[PubMed](#)]
72. Ross, M.F.; Kelso, G.F.; Blaikie, F.H.; James, A.M.; Cocheme, H.M.; Filipovska, A.; Da Ros, T.; Hurd, T.R.; Smith, R.A.J.; Murphy, M.P. Lipophilic triphenylphosphonium cations as tools in mitochondrial bioenergetics and free radical biology. *Biochemistry* **2005**, *70*, 222–230. [[CrossRef](#)] [[PubMed](#)]
73. Robinson, K.M.; Janes, M.S.; Pehar, M.; Monette, J.S.; Ross, M.F.; Hagen, T.M.; Murphy, M.P.; Beckman, J.S. Selective fluorescent imaging of superoxide in vivo using ethidium-based probes. *Proc. Natl. Acad. Sci. USA* **2006**, *103*, 15038–15043. [[CrossRef](#)] [[PubMed](#)]
74. Kauffman, M.E.; Kauffman, M.K.; Traore, K.; Zhu, H.; Trush, M.A.; Jia, Z.; Li, Y.R. MitoSOX-Based Flow Cytometry for Detecting Mitochondrial ROS. *React. Oxyg. Species* **2016**, *2*, 361–370. [[CrossRef](#)]
75. Mukhopadhyay, P.; Rajesh, M.; Yoshihiro, K.; Hasko, G.; Pacher, P. Simple quantitative detection of mitochondrial superoxide production in live cells. *BioChem. Biophys. Res. Commun.* **2007**, *358*, 203–208. [[CrossRef](#)] [[PubMed](#)]

76. Roelofs, B.A.; Ge, S.X.; Studlack, P.E.; Polster, B.M. Low micromolar concentrations of the superoxide probe MitoSOX uncouple neural mitochondria and inhibit complex IV. *Free Radic. Biol. Med.* **2015**, *86*, 250–258. [[CrossRef](#)]
77. Ohyashiki, T.; Nunomura, M.; Katoh, T. Detection of superoxide anion radical in phospholipid liposomal membrane by fluorescence quenching method using 1,3-diphenylisobenzofuran. *Bba-Biomembranes* **1999**, *1421*, 131–139. [[CrossRef](#)]
78. Krieg, M. Determination of singlet oxygen quantum yields with 1,3-diphenylisobenzofuran in model membrane systems. *J. BioChem. Biophys. Methods* **1993**, *27*, 143–149. [[CrossRef](#)]
79. Zamojc, K.; Zdrowowicz, M.; Rudnicki-Velasquez, P.B.; Krzyminski, K.; Zaborowski, B.; Niedzialkowski, P.; Jacewicz, D.; Chmurzynski, L. The development of 1,3-diphenylisobenzofuran as a highly selective probe for the detection and quantitative determination of hydrogen peroxide. *Free Radic. Res.* **2017**, *51*, 38–46. [[CrossRef](#)]
80. Andresen, M.; Regueira, T.; Bruhn, A.; Perez, D.; Strobel, P.; Dougnac, A.; Marshall, G.; Leighton, F. Lipoperoxidation and protein oxidative damage exhibit different kinetics during septic shock. *Mediat. Inflamm.* **2008**. [[CrossRef](#)] [[PubMed](#)]
81. Wu, D.F.; Cederbaum, A.I. Alcohol, oxidative stress, and free radical damage. *Alcohol. Res. Health* **2003**, *27*, 277–284. [[PubMed](#)]
82. Halliwell, B.; Chirico, S. Lipid-Peroxidation — Its Mechanism, Measurement, and Significance. *Am. J. Clin. Nutr.* **1993**, *57*, 715–725. [[CrossRef](#)] [[PubMed](#)]
83. Wang, X.; Zhang, L. Kinetic study of hydroxyl radical formation in a continuous hydroxyl generation system. *RSC Adv.* **2018**, *8*, 40632–40638. [[CrossRef](#)]
84. Kehrer, J.P. The Haber-Weiss reaction and mechanisms of toxicity. *Toxicology* **2000**, *149*, 43–50. [[CrossRef](#)]
85. Weinstein, J.; Bielski, B.H.J. Kinetics of the Interaction of HO₂ and O₂-Radicals with Hydrogen-Peroxide—Haber-Weiss Reaction. *J. Am. Chem. Soc.* **1979**, *101*, 58–62. [[CrossRef](#)]
86. Koppenol, W.H. The Haber-Weiss cycle—70 years later. *Redox Rep.* **2001**, *6*, 229–234. [[CrossRef](#)]
87. Fischbacher, A.; von Sonntag, C.; Schmidt, T.C. Hydroxyl radical yields in the Fenton process under various pH, ligand concentrations and hydrogen peroxide/Fe (II) ratios. *Chemosphere* **2017**, *182*, 738–744. [[CrossRef](#)]
88. Wang, T.; Zhang, H.; Liu, H.; Yuan, Q.; Ren, F.; Han, Y.; Sun, Q.; Li, Z.; Gao, M. Boosting H₂O₂-Guided Chemodynamic Therapy of Cancer by Enhancing Reaction Kinetics through Versatile Biomimetic Fenton Nanocatalysts and the Second Near-Infrared Light Irradiation. *Adv. Funct. Mater.* **2019**, *30*. [[CrossRef](#)]
89. Li, X.; Hao, S.J.; Han, A.L.; Yang, Y.Y.; Fang, G.Z.; Liu, J.F.; Wang, S. Intracellular Fenton reaction based on mitochondria-targeted copper (II)-peptide complex for induced apoptosis. *J. Mater. Chem. B* **2019**, *7*, 4008–4016. [[CrossRef](#)]
90. Hackenberg, S.; Scherzed, A.; Technau, A.; Kessler, M.; Froelich, K.; Ginzkey, C.; Koehler, C.; Burghartz, M.; Hagen, R.; Kleinsasser, N. Cytotoxic, genotoxic and pro-inflammatory effects of zinc oxide nanoparticles in human nasal mucosa cells in vitro. *Toxicol. In Vitro* **2011**, *25*, 657–663. [[CrossRef](#)]
91. Ekici, S.; Turkarlan, S.; Pawlik, G.; Dancis, A.; Baliga, N.S.; Koch, H.G.; Daldal, F. Intracytoplasmic copper homeostasis controls cytochrome c oxidase production. *mBio* **2014**, *5*. [[CrossRef](#)]
92. Huang, G.; Chen, H.; Dong, Y.; Luo, X.; Yu, H.; Moore, Z.; Bey, E.A.; Boothman, D.A.; Gao, J. Superparamagnetic iron oxide nanoparticles: Amplifying ROS stress to improve anticancer drug efficacy. *Theranostics* **2013**, *3*, 116–126. [[CrossRef](#)] [[PubMed](#)]
93. Lehman, S.E.; Morris, A.S.; Mueller, P.S.; Salem, A.K.; Grassian, V.H.; Larsen, S.C. Silica nanoparticle-generated ROS as a predictor of cellular toxicity: Mechanistic insights and safety by design. *Environ. Sci-Nano* **2016**, *3*, 56–66. [[CrossRef](#)]
94. Chairuangkitti, P.; Lawanprasert, S.; Roytrakul, S.; Aueviriyavit, S.; Phummiratch, D.; Kulthong, K.; Chanvorachote, P.; Maniratanachote, R. Silver nanoparticles induce toxicity in A549 cells via ROS-dependent and ROS-independent pathways. *Toxicol. In Vitro* **2013**, *27*, 330–338. [[CrossRef](#)] [[PubMed](#)]
95. Fang, X.W.; Mark, G.; von Sonntag, C. OH radical formation by ultrasound in aqueous solutions Part I: The chemistry underlying the terephthalate dosimeter. *Ultrason. Sonochem.* **1996**, *3*, 57–63. [[CrossRef](#)]
96. Yan, E.B.; Unthank, J.K.; Castillo-Melendez, M.; Miller, S.L.; Langford, S.J.; Walker, D.W. Novel method for in vivo hydroxyl radical measurement by microdialysis in fetal sheep brain in utero. *J. Appl. Physiol.* **2005**, *98*, 2304–2310. [[CrossRef](#)] [[PubMed](#)]
97. Yapici, N.B.; Jockusch, S.; Moscatelli, A.; Mandalapu, S.R.; Itagaki, Y.; Bates, D.K.; Wiseman, S.; Gibson, K.M.; Turro, N.J.; Bi, L.R. New Rhodamine Nitroxide Based Fluorescent Probes for Intracellular Hydroxyl Radical Identification in Living Cells. *Org. Lett.* **2012**, *14*, 50–53. [[CrossRef](#)]
98. Bai, X.Y.; Huang, Y.Y.; Lu, M.Y.; Yang, D. HKOH-1: A Highly Sensitive and Selective Fluorescent Probe for Detecting Endogenous Hydroxyl Radicals in Living Cells. *Angew. Chem. Int. Ed.* **2017**, *56*, 12873–12877. [[CrossRef](#)]
99. Cheng, X.; Guo, H.; Zhang, Y.; Wu, X.; Liu, Y. Non-photochemical production of singlet oxygen via activation of persulfate by carbon nanotubes. *Water Res.* **2017**, *113*, 80–88. [[CrossRef](#)] [[PubMed](#)]
100. Cadenas, E. Biochemistry of Oxygen-Toxicity. *Annu. Rev. BioChem.* **1989**, *58*, 79–110. [[CrossRef](#)] [[PubMed](#)]
101. Agnez-Lima, L.F.; Melo, J.T.A.; Silva, A.E.; Oliveira, A.H.S.; Timoteo, A.R.S.; Lima-Bessa, K.M.; Martinez, G.R.; Medeiros, M.H.G.; Di Mascio, P.; Galhardo, R.S.; et al. DNA damage by singlet oxygen and cellular protective mechanisms. *Mutat. Res. Rev. Mutat.* **2012**, *751*, 15–28. [[CrossRef](#)] [[PubMed](#)]
102. Hampton, M.B.; Kettle, A.J.; Winterbourn, C.C. Inside the neutrophil phagosome: Oxidants, myeloperoxidase, and bacterial killing. *Blood* **1998**, *92*, 3007–3017. [[CrossRef](#)] [[PubMed](#)]
103. Bigot, E.; Bataille, R.; Patrice, T. Increased singlet oxygen-induced secondary ROS production in the serum of cancer patients. *J. PhotoChem. PhotoBiol. B* **2012**, *107*, 14–19. [[CrossRef](#)]
104. Sies, H.; Menck, C.F.M. Singlet Oxygen Induced DNA Damage. *Mutat Res.* **1992**, *275*, 367–375. [[CrossRef](#)]

105. Kanofsky, J.R. Singlet Oxygen Production by Biological-Systems. *Chem. Biol. Interact.* **1989**, *70*, 1–28. [[CrossRef](#)]
106. Dumont, E.; Gruber, R.; Bignon, E.; Morell, C.; Moreau, Y.; Monari, A.; Ravanat, J.L. Probing the reactivity of singlet oxygen with purines. *Nucleic Acids Res.* **2016**, *44*, 56–62. [[CrossRef](#)] [[PubMed](#)]
107. Davies, M.J. Singlet oxygen-mediated damage to proteins and its consequences. *BioChem. Biophys. Res. Commun.* **2003**, *305*, 761–770. [[CrossRef](#)]
108. Gracanin, M.; Hawkins, C.L.; Pattison, D.I.; Davies, M.J. Singlet-oxygen-mediated amino acid and protein oxidation: Formation of tryptophan peroxides and decomposition products. *Free Radic. Bio Med.* **2009**, *47*, 92–102. [[CrossRef](#)]
109. Hirakawa, T.; Nosaka, Y. Properties of $O_2^{\cdot -}$ and OH center dot formed in TiO₂ aqueous suspensions by photocatalytic reaction and the influence of H₂O₂ and some ions. *Langmuir* **2002**, *18*, 3247–3254. [[CrossRef](#)]
110. Kim, S.Y.; Lee, S.M.; Park, J.W. Antioxidant enzyme inhibitors enhance singlet oxygen-induced cell death in HL-60 cells. *Free Radic. Res.* **2006**, *40*, 1190–1197. [[CrossRef](#)] [[PubMed](#)]
111. Deng, J.; Liu, F.; Wang, L.; An, Y.; Gao, M.; Wang, Z.; Zhao, Y. Hypoxia- and singlet oxygen-responsive chemo-photodynamic Micelles featured with glutathione depletion and aldehyde production. *Biomater. Sci.* **2018**, *7*, 429–441. [[CrossRef](#)]
112. Kim, S.Y.; Lee, S.M.; Tak, J.K.; Choi, K.S.; Kwon, T.K.; Park, J.W. Regulation of singlet oxygen-induced apoptosis by cytosolic NADP⁺-dependent isocitrate dehydrogenase. *Mol. Cell Biochem.* **2007**, *302*, 27–34. [[CrossRef](#)]
113. Umezawa, N.; Tanaka, K.; Urano, Y.; Kikuchi, K.; Higuchi, T.; Nagano, T. Novel Fluorescent Probes for Singlet Oxygen. *Angew. Chem. Int. Ed. Engl.* **1999**, *38*, 2899–2901. [[CrossRef](#)]
114. Brega, V.; Yan, Y.; Thomas, S.W., 3rd. Acenes beyond organic electronics: Sensing of singlet oxygen and stimuli-responsive materials. *Org. Biomol. Chem.* **2020**, *18*, 9191–9209. [[CrossRef](#)] [[PubMed](#)]
115. Ruiz-Gonzalez, R.; Bresoli-Obach, R.; Gulias, O.; Agut, M.; Savoie, H.; Boyle, R.W.; Nonell, S.; Giuntini, F. NanoSOSG: A Nanostructured Fluorescent Probe for the Detection of Intracellular Singlet Oxygen. *Angew. Chem. Int. Ed. Engl.* **2017**, *56*, 2885–2888. [[CrossRef](#)]
116. Lennicke, C.; Rahn, J.; Lichtenfels, R.; Wessjohann, L.A.; Seliger, B. Hydrogen peroxide—Production, fate and role in redox signaling of tumor cells. *Cell Commun. Signal.* **2015**, *13*, 39. [[CrossRef](#)] [[PubMed](#)]
117. Hossain, M.A.; Bhattacharjee, S.; Armin, S.M.; Qian, P.; Xin, W.; Li, H.Y.; Burritt, D.J.; Fujita, M.; Tran, L.S. Hydrogen peroxide priming modulates abiotic oxidative stress tolerance: Insights from ROS detoxification and scavenging. *Front. Plant. Sci.* **2015**, *6*, 420. [[CrossRef](#)] [[PubMed](#)]
118. Halliwell, B.; Clement, M.V.; Long, L.H. Hydrogen peroxide in the human body. *FEBS Lett.* **2000**, *486*, 10–13. [[CrossRef](#)]
119. Mates, J.M.; Perez-Gomez, C.; De Castro, I.N. Antioxidant enzymes and human diseases. *Clin. Biochem.* **1999**, *32*, 595–603. [[CrossRef](#)]
120. Angermuller, S.; Islinger, M.; Volkl, A. Peroxisomes and reactive oxygen species, a lasting challenge. *HistoChem. Cell Biol.* **2009**, *131*, 459–463. [[CrossRef](#)]
121. Topo, E.; Fisher, G.; Sorricelli, A.; Errico, F.; Usiello, A.; D’Aniello, A. Thyroid hormones and D-aspartic acid, D-aspartate oxidase, D-aspartate racemase, H₂O₂, and ROS in rats and mice. *Chem. Biodivers.* **2010**, *7*, 1467–1478. [[CrossRef](#)] [[PubMed](#)]
122. Royall, J.A.; Ischiropoulos, H. Evaluation of 2',7'-Dichlorofluorescein and Dihydrorhodamine 123 as Fluorescent-Probes for Intracellular H₂O₂ in Cultured Endothelial-Cells. *Arch. Biochem. Biophys.* **1993**, *302*, 348–355. [[CrossRef](#)] [[PubMed](#)]
123. Rastogi, R.P.; Singh, S.P.; Hader, D.P.; Sinha, R.P. Detection of reactive oxygen species (ROS) by the oxidant-sensing probe 2',7'-dichlorodihydrofluorescein diacetate in the cyanobacterium *Anabaena variabilis* PCC 7937. *Biochem. Biophys. Res. Commun.* **2010**, *397*, 603–607. [[CrossRef](#)] [[PubMed](#)]
124. Gomes, A.; Fernandes, E.; Lima, J.L.F.C. Fluorescence probes used for detection of reactive oxygen species. *J. Biochem. Biophys Meth.* **2005**, *65*, 45–80. [[CrossRef](#)]
125. Crow, J.P. Dichlorodihydrofluorescein and dihydrorhodamine 123 are sensitive indicators of peroxynitrite in vitro: Implications for intracellular measurement of reactive nitrogen and oxygen species. *Nitric Oxide* **1997**, *1*, 145–157. [[CrossRef](#)]
126. Chignell, C.F.; Sik, R.H. A photochemical study of cells loaded with 2',7'-dichlorofluorescein: Implications for the detection of reactive oxygen species generated during UVA irradiation. *Free Radic. Biol. Med.* **2003**, *34*, 1029–1034. [[PubMed](#)]
127. Zhu, H.; Bannenberg, G.L.; Moldeus, P.; Shertzer, H.G. Oxidation pathways for the intracellular probe 2',7'-dichlorofluorescein. *Arch. Toxicol.* **1994**, *68*, 582–587. [[CrossRef](#)]
128. Lebel, C.P.; Ischiropoulos, H.; Bondy, S.C. Evaluation of the Probe 2',7'-Dichlorofluorescein as an Indicator of Reactive Oxygen Species Formation and Oxidative Stress. *Chem. Res. Toxicol.* **1992**, *5*, 227–231. [[CrossRef](#)]
129. Hsiao, I.L.; Huang, Y.J. Titanium Oxide Shell Coatings Decrease the Cytotoxicity of ZnO Nanoparticles. *Chem. Res. Toxicol.* **2011**, *24*, 303–313. [[CrossRef](#)] [[PubMed](#)]
130. Akhtar, M.J.; Ahamed, M.; Kumar, S.; Khan, M.M.; Ahmad, J.; Alrokayan, S.A. Zinc oxide nanoparticles selectively induce apoptosis in human cancer cells through reactive oxygen species. *Int. J. Nanomed.* **2012**, *7*, 845–857.
131. Sharma, V.; Anderson, D.; Dhawan, A. Zinc oxide nanoparticles induce oxidative DNA damage and ROS-triggered mitochondria mediated apoptosis in human liver cells (HepG2). *Apoptosis* **2012**, *17*, 852–870. [[CrossRef](#)] [[PubMed](#)]
132. Setyawati, M.I.; Tay, C.Y.; Leong, D.T. Effect of zinc oxide nanomaterials-induced oxidative stress on the p53 pathway. *Biomaterials* **2013**, *34*, 10133–10142. [[CrossRef](#)]

133. Aliakbari, F.; Haji Hosseinali, S.; Khalili Sarokhalil, Z.; Shahpasand, K.; Akbar Saboury, A.; Akhtari, K.; Falahati, M. Reactive oxygen species generated by titanium oxide nanoparticles stimulate the hemoglobin denaturation and cytotoxicity against human lymphocyte cell. *J. Biomol. Struct. Dyn.* **2019**, *37*, 4875–4881. [[CrossRef](#)] [[PubMed](#)]
134. Bhattacharya, K.; Davoren, M.; Boertz, J.; Schins, R.P.; Hoffmann, E.; Dopp, E. Titanium dioxide nanoparticles induce oxidative stress and DNA-adduct formation but not DNA-breakage in human lung cells. *Part. Fibre Toxicol.* **2009**, *6*, 17. [[CrossRef](#)]
135. Liu, S.; Xu, L.; Zhang, T.; Ren, G.; Yang, Z. Oxidative stress and apoptosis induced by nanosized titanium dioxide in PC12 cells. *Toxicology* **2010**, *267*, 172–177. [[CrossRef](#)] [[PubMed](#)]
136. Park, E.J.; Yi, J.; Chung, K.H.; Ryu, D.Y.; Choi, J.; Park, K. Oxidative stress and apoptosis induced by titanium dioxide nanoparticles in cultured BEAS-2B cells. *Toxicol. Lett.* **2008**, *180*, 222–229. [[CrossRef](#)] [[PubMed](#)]
137. Miwa, S.; Treumann, A.; Bell, A.; Vistoli, G.; Nelson, G.; Hay, S.; von Zglinicki, T. Carboxylesterase converts Amplex red to resorufin: Implications for mitochondrial H₂O₂ release assays. *Free Radic. Biol. Med.* **2016**, *90*, 173–183. [[CrossRef](#)] [[PubMed](#)]
138. Zhu, A.; Romero, R.; Petty, H.R. A sensitive fluorimetric assay for pyruvate. *Anal. Biochem.* **2010**, *396*, 146–151. [[CrossRef](#)] [[PubMed](#)]
139. Towne, V.; Will, M.; Oswald, B.; Zhao, Q.J. Complexities in horseradish peroxidase-catalyzed oxidation of dihydroxyphenoxazine derivatives: Appropriate ranges for pH values and hydrogen peroxide concentrations in quantitative analysis. *Anal. Biochem.* **2004**, *334*, 290–296. [[CrossRef](#)] [[PubMed](#)]
140. Debski, D.; Smulik, R.; Zielonka, J.; Michalowski, B.; Jakubowska, M.; Debowska, K.; Adamus, J.; Marcinek, A.; Kalyanaraman, B.; Sikora, A. Mechanism of oxidative conversion of Amplex (R) Red to resorufin: Pulse radiolysis and enzymatic studies. *Free Radic. Bio Med.* **2016**, *95*, 323–332. [[CrossRef](#)]
141. Niethammer, P.; Grabher, C.; Look, A.T.; Mitchison, T.J. A tissue-scale gradient of hydrogen peroxide mediates rapid wound detection in zebrafish. *Nature* **2009**, *459*, 996–999. [[CrossRef](#)] [[PubMed](#)]
142. Maeda, H.; Fukuyasu, Y.; Yoshida, S.; Fukuda, M.; Saeki, K.; Matsuno, H.; Yamauchi, Y.; Yoshida, K.; Hirata, K.; Miyamoto, K. Fluorescent probes for hydrogen peroxide based on a non-oxidative mechanism. *Angew. Chem. Int. Ed. Engl.* **2004**, *43*, 2389–2391. [[CrossRef](#)] [[PubMed](#)]
143. Wolfbeis, O.S.; Durkop, A.; Wu, M.; Lin, Z.H. A europium-ion-based luminescent sensing probe for hydrogen peroxide. *Angew. Chem. Int. Ed.* **2002**, *41*, 4495–4498. [[CrossRef](#)]
144. Staniek, K.; Nohl, H. H₂O₂ detection from intact mitochondria as a measure for one-electron reduction of dioxygen requires a non-invasive assay system. *Bba-Bioenergetics* **1999**, *1413*, 70–80. [[CrossRef](#)]
145. Bartosz, G. Use of spectroscopic probes for detection of reactive oxygen species. *Clin. Chim. Acta* **2006**, *368*, 53–76. [[CrossRef](#)] [[PubMed](#)]
146. Mohammadinejad, R.; Moosavi, M.A.; Tavakol, S.; Vardar, D.O.; Hosseini, A.; Rahmati, M.; Dini, L.; Hussain, S.; Mandegary, A.; Klionsky, D.J. Necrotic, apoptotic and autophagic cell fates triggered by nanoparticles. *Autophagy* **2019**, *15*, 4–33. [[CrossRef](#)] [[PubMed](#)]
147. Mittler, R.; Vanderauwera, S.; Suzuki, N.; Miller, G.; Tognetti, V.B.; Vandepoele, K.; Gollery, M.; Shulaev, V.; Van Breusegem, F. ROS signaling: The new wave? *Trends Plant. Sci.* **2011**, *16*, 300–309. [[CrossRef](#)] [[PubMed](#)]
148. Zhang, J.; Wang, X.; Vikash, V.; Ye, Q.; Wu, D.; Liu, Y.; Dong, W. ROS and ROS-Mediated Cellular Signaling. *Oxid Med. Cell Longev.* **2016**. [[CrossRef](#)] [[PubMed](#)]
149. Bae, Y.S.; Oh, H.; Rhee, S.G.; Yoo, Y.D. Regulation of reactive oxygen species generation in cell signaling. *Mol. Cells* **2011**, *32*, 491–509. [[CrossRef](#)]
150. Bonizzi, G.; Karin, M. The two NF-kappaB activation pathways and their role in innate and adaptive immunity. *Trends Immunol.* **2004**, *25*, 280–288. [[CrossRef](#)]
151. Kaul, N.; Gopalakrishna, R.; Gundimeda, U.; Choi, J.; Forman, H.J. Role of protein kinase C in basal and hydrogen peroxide-stimulated NF-kappa B activation in the murine macrophage J774A.1 cell line. *Arch. Biochem. Biophys.* **1998**, *350*, 79–86. [[CrossRef](#)] [[PubMed](#)]
152. Schmidt, K.N.; Amstad, P.; Cerutti, P.; Baeuerle, P.A. The roles of hydrogen peroxide and superoxide as messengers in the activation of transcription factor NF-kappa B. *Chem. Biol.* **1995**, *2*, 13–22. [[CrossRef](#)]
153. Schoonbroodt, S.; Ferreira, V.; Best-Belpomme, M.; Boelaert, J.R.; Legrand-Poels, S.; Korner, M.; Piette, J. Crucial role of the amino-terminal tyrosine residue 42 and the carboxyl-terminal PEST domain of I kappa B alpha in NF-kappa B activation by an oxidative stress. *J. Immunol.* **2000**, *164*, 4292–4300. [[CrossRef](#)] [[PubMed](#)]
154. Takada, Y.; Mukhopadhyay, A.; Kundu, G.C.; Mahabeleshwar, G.H.; Singh, S.; Aggarwal, B.B. Hydrogen peroxide activates NF-kappa B through tyrosine phosphorylation of I kappa B alpha and serine phosphorylation of p65: Evidence for the involvement of I kappa B alpha kinase and Syk protein-tyrosine kinase. *J. Biol. Chem.* **2003**, *278*, 24233–24241. [[CrossRef](#)]
155. Liu, X.; Lu, B.; Fu, J.; Zhu, X.; Song, E.; Song, Y. Amorphous silica nanoparticles induce inflammation via activation of NLRP3 inflammasome and HMGB1/TLR4/MYD88/NF-kb signaling pathway in HUVEC cells. *J. Hazard. Mater.* **2021**, *404*, 124050. [[CrossRef](#)] [[PubMed](#)]
156. Kyriakis, J.M.; Avruch, J. Sounding the alarm: Protein kinase cascades activated by stress and inflammation. *J. Biol. Chem.* **1996**, *271*, 24313–24316. [[CrossRef](#)]
157. Nakano, H.; Nakajima, A.; Sakon-Komazawa, S.; Piao, J.H.; Xue, X.; Okumura, K. Reactive oxygen species mediate crosstalk between NF-kappaB and JNK. *Cell Death Differ.* **2006**, *13*, 730–737. [[CrossRef](#)]

158. Torres, M.; Forman, H.J. Redox signaling and the MAP kinase pathways. *Biofactors* **2003**, *17*, 287–296. [[CrossRef](#)] [[PubMed](#)]
159. Dabrowski, A.; Boguslowicz, C.; Dabrowska, M.; Tribillo, I.; Gabryelewicz, A. Reactive oxygen species activate mitogen-activated protein kinases in pancreatic acinar cells. *Pancreas* **2000**, *21*, 376–384. [[CrossRef](#)]
160. Guyton, K.Z.; Liu, Y.; Gorospe, M.; Xu, Q.; Holbrook, N.J. Activation of mitogen-activated protein kinase by H₂O₂. Role in cell survival following oxidant injury. *J. Biol. Chem.* **1996**, *271*, 4138–4142. [[CrossRef](#)] [[PubMed](#)]
161. Hou, N.; Torii, S.; Saito, N.; Hosaka, M.; Takeuchi, T. Reactive oxygen species-mediated pancreatic beta-cell death is regulated by interactions between stress-activated protein kinases, p38 and c-Jun N-terminal kinase, and mitogen-activated protein kinase phosphatases. *Endocrinology* **2008**, *149*, 1654–1665. [[CrossRef](#)] [[PubMed](#)]
162. Choi, B.H.; Hur, E.M.; Lee, J.H.; Jun, D.J.; Kim, K.T. Protein kinase Cdelta-mediated proteasomal degradation of MAP kinase phosphatase-1 contributes to glutamate-induced neuronal cell death. *J. Cell Sci.* **2006**, *119*, 1329–1340. [[CrossRef](#)] [[PubMed](#)]
163. Matsuzawa, A.; Saegusa, K.; Noguchi, T.; Sadamitsu, C.; Nishitoh, H.; Nagai, S.; Koyasu, S.; Matsumoto, K.; Takeda, K.; Ichijo, H. ROS-dependent activation of the TRAF6-ASK1-p38 pathway is selectively required for TLR4-mediated innate immunity. *Nat. Immunol.* **2005**, *6*, 587–592. [[CrossRef](#)] [[PubMed](#)]
164. Pitzschke, A.; Djamei, A.; Bitton, F.; Hirt, H. A Major Role of the MEKK1-MKK1/2-MPK4 Pathway in ROS Signalling. *Mol. Plant.* **2009**, *2*, 120–137. [[CrossRef](#)] [[PubMed](#)]
165. Lluis, J.M.; Buricchi, F.; Chiarugi, P.; Morales, A.; Fernandez-Checa, J.C. Dual role of mitochondrial reactive oxygen species in hypoxia signaling: Activation of nuclear factor- κ B via c-SRC and oxidant-dependent cell death. *Cancer Res.* **2007**, *67*, 7368–7377. [[CrossRef](#)] [[PubMed](#)]
166. Dong, J.; Ramachandiran, S.; Tikoo, K.; Jia, Z.; Lau, S.S.; Monks, T.J. EGFR-independent activation of p38 MAPK and EGFR-dependent activation of ERK1/2 are required for ROS-induced renal cell death. *Am. J. Physiol. Renal Physiol.* **2004**, *287*, 1049–1058. [[CrossRef](#)] [[PubMed](#)]
167. Forman, H.J.; Torres, M. Reactive oxygen species and cell signaling: Respiratory burst in macrophage signaling. *Am. J. Respir. Crit. Care Med.* **2002**, *166*. [[CrossRef](#)]
168. Cheng, G.; Guo, W.; Han, L.; Chen, E.; Kong, L.; Wang, L.; Ai, W.; Song, N.; Li, H.; Chen, H. Cerium oxide nanoparticles induce cytotoxicity in human hepatoma SMMC-7721 cells via oxidative stress and the activation of MAPK signaling pathways. *Toxicol. In Vitro* **2013**, *27*, 1082–1088. [[CrossRef](#)] [[PubMed](#)]
169. Guo, C.; Xia, Y.; Niu, P.; Jiang, L.; Duan, J.; Yu, Y.; Zhou, X.; Li, Y.; Sun, Z. Silica nanoparticles induce oxidative stress, inflammation, and endothelial dysfunction in vitro via activation of the MAPK/Nrf2 pathway and nuclear factor-kappaB signaling. *Int. J. Nanomed.* **2015**, *10*, 1463–1477. [[CrossRef](#)]
170. You, R.; Ho, Y.S.; Hung, C.H.; Liu, Y.; Huang, C.X.; Chan, H.N.; Ho, S.L.; Lui, S.Y.; Li, H.W.; Chang, R.C. Silica nanoparticles induce neurodegeneration-like changes in behavior, neuropathology, and affect synapse through MAPK activation. *Part. Fibre Toxicol.* **2018**, *15*, 28. [[CrossRef](#)]
171. Hu, Q.; Wang, H.; He, C.; Jin, Y.; Fu, Z. Polystyrene nanoparticles trigger the activation of p38 MAPK and apoptosis via inducing oxidative stress in zebrafish and macrophage cells. *Environ. Pollut.* **2021**, *269*, 116075. [[CrossRef](#)] [[PubMed](#)]
172. Zhou, Y.; Ji, J.; Ji, L.; Wang, L.; Hong, F. Respiratory exposure to nano-TiO₂ induces pulmonary toxicity in mice involving reactive free radical-activated TGF-beta/Smad/p38MAPK/Wnt pathways. *J. Biomed. Mater. Res. A* **2019**, *107*, 2567–2575. [[CrossRef](#)] [[PubMed](#)]
173. Yi, C.; Liu, D.; Fong, C.C.; Zhang, J.; Yang, M. Gold nanoparticles promote osteogenic differentiation of mesenchymal stem cells through p38 MAPK pathway. *ACS Nano* **2010**, *4*, 6439–6448. [[CrossRef](#)] [[PubMed](#)]
174. Wang, Q.; Chen, B.; Cao, M.; Sun, J.; Wu, H.; Zhao, P.; Xing, J.; Yang, Y.; Zhang, X.; Ji, M.; et al. Response of MAPK pathway to iron oxide nanoparticles in vitro treatment promotes osteogenic differentiation of hBMSCs. *Biomaterials* **2016**, *86*, 11–20. [[CrossRef](#)] [[PubMed](#)]
175. Vousden, K.H.; Lu, X. Live or let die: The cell's response to p53. *Nat. Rev. Cancer* **2002**, *2*, 594–604. [[CrossRef](#)]
176. Liu, B.; Chen, Y.; St Clair, D.K. ROS and p53: A versatile partnership. *Free Radic. Biol. Med.* **2008**, *44*, 1529–1535. [[CrossRef](#)]
177. Song, Y.X.; Li, X.W.; Li, Y.; Li, N.; Shi, X.X.; Ding, H.Y.; Zhang, Y.H.; Li, X.B.; Liu, G.W.; Wang, Z. Non-esterified fatty acids activate the ROS-p38-p53/Nrf2 signaling pathway to induce bovine hepatocyte apoptosis in vitro. *Apoptosis* **2014**, *19*, 984–997. [[CrossRef](#)] [[PubMed](#)]
178. Nakano, K.; Vousden, K.H. PUMA, a novel proapoptotic gene, is induced by p53. *Mol. Cell* **2001**, *7*, 683–694. [[CrossRef](#)]
179. Liu, B.R.; Yuan, B.; Zhang, L.; Mu, W.M.; Wang, C.M. ROS/p38/p53/Puma signaling pathway is involved in emodin-induced apoptosis of human colorectal cancer cells. *Int. J. Clin. Exp. Med.* **2015**, *8*, 15413–15422. [[PubMed](#)]
180. Yu, J.; Zhang, L. PUMA, a potent killer with or without p53. *Oncogene* **2008**, *27*, 71–83. [[CrossRef](#)] [[PubMed](#)]
181. Samuelson, J.T.; Dahl, J.E.; Karlsson, S.; Morisbak, E.; Becher, R. Apoptosis induced by the monomers HEMA and TEGDMA involves formation of ROS and differential activation of the MAP-kinases p38, JNK and ERK. *Dent. Mater.* **2007**, *23*, 34–39. [[CrossRef](#)]
182. Sakon, S.; Xue, X.; Takekawa, M.; Sasazuki, T.; Okazaki, T.; Kojima, Y.; Piao, J.H.; Yagita, H.; Okumura, K.; Doi, T.; et al. NF-kappaB inhibits TNF-induced accumulation of ROS that mediate prolonged MAPK activation and necrotic cell death. *Embo J.* **2003**, *22*, 3898–3909. [[CrossRef](#)] [[PubMed](#)]
183. Kamata, H.; Honda, S.; Maeda, S.; Chang, L.; Hirata, H.; Karin, M. Reactive oxygen species promote TNFalpha-induced death and sustained JNK activation by inhibiting MAP kinase phosphatases. *Cell* **2005**, *120*, 649–661. [[CrossRef](#)] [[PubMed](#)]

184. Akcan, R.; Aydogan, H.C.; Yildirim, M.S.; Tastekin, B.; Saglam, N. Nanotoxicity: A challenge for future medicine. *Turk. J. Med. Sci.* **2020**, *50*, 1180–1196. [[CrossRef](#)] [[PubMed](#)]
185. Graham, U.M.; Dozier, A.K.; Oberdorster, G.; Yokel, R.A.; Molina, R.; Brain, J.D.; Pinto, J.M.; Weuve, J.; Bennett, D.A. Tissue Specific Fate of Nanomaterials by Advanced Analytical Imaging Techniques—A Review. *Chem. Res. Toxicol.* **2020**, *33*, 1145–1162. [[CrossRef](#)] [[PubMed](#)]
186. Pu, S.; Gong, C.; Robertson, A.W. Liquid cell transmission electron microscopy and its applications. *R. Soc. Open Sci.* **2020**, *7*, 191204. [[CrossRef](#)]
187. Kiio, T.M.; Park, S. Nano-scientific Application of Atomic Force Microscopy in Pathology: From Molecules to Tissues. *Int. J. Med. Sci.* **2020**, *17*, 844–858. [[CrossRef](#)] [[PubMed](#)]
188. Erofeev, A.; Gorelkin, P.; Garanina, A.; Alova, A.; Efremova, M.; Vorobyeva, N.; Edwards, C.; Korchev, Y.; Majouga, A. Novel method for rapid toxicity screening of magnetic nanoparticles. *Sci. Rep.* **2018**, *8*, 7462. [[CrossRef](#)]
189. Rahman, L.; Williams, A.; Gelda, K.; Nikota, J.; Wu, D.; Vogel, U.; Halappanavar, S. 21st Century Tools for Nanotoxicology: Transcriptomic Biomarker Panel and Precision-Cut Lung Slice Organ Mimic System for the Assessment of Nanomaterial-Induced Lung Fibrosis. *Small* **2020**, *16*. [[CrossRef](#)]
190. Kohl, Y.; Runden-Pran, E.; Mariussen, E.; Hesler, M.; El Yamani, N.; Longhin, E.M.; Dusinska, M. Genotoxicity of Nanomaterials: Advanced In Vitro Models and High Throughput Methods for Human Hazard Assessment-A Review. *Nanomaterials (Basel)* **2020**, *10*, 1911. [[CrossRef](#)] [[PubMed](#)]
191. Zhang, M.; Xu, C.; Jiang, L.; Qin, J. A 3D human lung-on-a-chip model for nanotoxicity testing. *Toxicol. Res.* **2018**, *7*, 1048–1060. [[CrossRef](#)] [[PubMed](#)]
192. Yin, F.; Zhu, Y.; Zhang, M.; Yu, H.; Chen, W.; Qin, J. A 3D human placenta-on-a-chip model to probe nanoparticle exposure at the placental barrier. *Toxicol. In Vitro* **2019**, *54*, 105–113. [[CrossRef](#)] [[PubMed](#)]
193. van Duinen, V.; Trietsch, S.J.; Joore, J.; Vulto, P.; Hankemeier, T. Microfluidic 3D cell culture: From tools to tissue models. *Curr. Opin. Biotechnol.* **2015**, *35*, 118–126. [[CrossRef](#)] [[PubMed](#)]